University of Technology, Sydney

Model Predictive Control of DFIG-Based Wind Turbine

Degree of Master of Engineering

(By Research)

in the
Faculty of Engineering and Information Technology

School of Electrical, Mechanical and Mechatronic Systems

By: Ehsan Gatavi

Superviser: Professor Tuan Hoang

October 2014

CERTIFICATE OF ORIGINAL AUTHORSHIP

I certify that the work in this thesis has not previously been submitted for a degree nor has it been submitted as part of requirements for a degree except as fully acknowledged within the text.
I also certify that the thesis has been written by me. Any help that I have received in my research work and the preparation of the thesis itself has been acknowledged. In addition, I certify that all information sources and literature used are indicated in the thesis.

Signature of Student: *Ehsan Gatavi*

Date: *7 Ocotber 2014*

Acknowledgements

I would like to express my sincere thanks and appreciation to Professor H. D. Tuan, my advisor for his continuous guidance, financial support, patience, and encouragement throughout my research work. His technical and editorial advice has been essential for the completion of this thesis. Despite of his busy schedule, he always manages to prepare a meeting when there is a need.

I am thankful to the Center of Health Technologies and School of Electrical, Mechanical and Mechatronic members at UTS for contributing to such a pleasant atmosphere.

The librarians at University of Technology Sydney deserve special thanks for their assistance in supplying the relevant literatures.

Finally, my deepest appreciation goes to my parents for their support, never-ending patience, and inspiration who endured this long process with me, always offering support and love.

Contents

List of Tables

List of Figures

Abbreviations

RET	Renewable Energy Target
VFC	Variable Frequency Converter
WT	Wind Turbine
WF	Wind Farm
DFIG	Doubly Fed Induction Generator
QP	Quadratic Programming
PI	Proportional Integral
LQG	Linear Quadratic Gaussian
MPC	Model Predictive Control
DMPC	Decentralised Model Predictive Control
CO_2	Carbon Dioxide
RSC	Rotor Side Converter
GSC	Grid Side Converter
SDR	Series Dynamic Resistor
NSW	New South Wales
HAWT	Horizontal Axis Wind Turbine
TSR	Tip Speed Ratio
PSF	Power Signal Feedback
MPPT	Maximum Power Point Tracking
SCIG	Squirrel Cage Induction Generator
WRIG	Wound Rotor Induction Generator
PMSG	Permanent Magnet Synchronous Generator
WRSG	Wound Rotor Synchronous Generator
WECS	Wind Energy Conversion System
WTGS	Wind Turbine Generator System
ORC	Optimal Regime Characteristic
MW	Mega Watt
MIMO	Multi-Input-Multi-Output
LVRT	Low Voltage Ride Through
HVRT	High Voltage Ride Through

Abbreviations

FRT	Fault Ride Through
STATCOM	Static synchronous Compensator
UK	United Kingdom
PCC	Point Common Coupling
IGBT	Insulated Gate Bipolar Transistors
GTO	Gate Turn-Off Thyristors
PWM	Pulse Width Modulation
APRC	Asymptotically Positive Realness Constraint

Abstract

Renewable energy as a green source of energy is clean, accessible and sustainable. Due to advanced control, lower cost and government incentives, wind energy has been the largest growth among other renewable sources.

With fast growing in the new generation of generators, Doubly Fed Induction Generators (DFIGs) became more popular because of handling a fraction (20-30%) of the total system power which leads to reduce the losses in the power electronic equipment and also their ability in decoupling the control of both active and reactive power. In addition, DFIGs have better behaviour in system stability. Therefore, in this study, the model of one-mass wind turbine with DFIG is represented by a third order model.

Model Predictive Control (MPC), as a powerful control method to handle multivariable systems and incorporate constraints, is applied in order to compensate inaccuracies and measurement noise. The optimization problem is recast as a Quadratic Programming (QP) which is highly robust and efficient. Multi-step optimization is introduced to bring the unhealthy voltages as close as possible to the normal operating points so that leads to minimize the changes of the control variables.

In order to regulate the power flow between the grid and the generator, it is essential to update reactive power with real power and actual terminal voltage besides reaching maximum reactive power. In this study, the updated control input applies feedback to MPC at each control step by solving a new optimization problem.

Chapter 1

Importance of Wind Energy

1.1 Introduction

Wind power is a good renewable, clean and free source of energy for power production. Due to the concern about the environmental pollution and reducing dependence on fossil fuels and CO_2 emissions, there has been a rapid increase in renewable energy and especially wind energy in the last decade [1].
One of the key challenging issues is that a wind farm has to provide fault ride through capability and remains connected during network faults [2]. However, in the fast development of wind turbine techniques, wind turbines with Doubly Fed Induction Generator (DFIG) is becoming the dominant type of wind turbine systems used in wind farms.
The most important benefit of DFIG, is its capability of handling 20-30% of the total system power which leads to reduce the losses in the power electronic equipment [3]. Moreover, because of DFIG's capability in decoupling the control of power (both active and reactive), these types of generators have better behaviour in system stability during short circuit faults compared with induction generators.
In the case that the power rating in variable frequency ac/dc/ac converter (VFC) is only 25%-30% of the induction generator power rating, over current can lead to the destruction of the converter [1]. Furthermore, even faults in a power system far away from the location of wind turbine lead to a voltage dip at the connection point of generator [4].
Doubly Fed Induction Generator (DFIG) is connected to the grid through Rotor Side Converter (RSC). [5] has stated that the sensitivity of DFIGs to change in their terminal voltage is the main drawback of this equipment. This weakness leads to the destruction of the RSC, especially when an external fault occurs. Typical solution for industrial application is using crowbar protection. The disadvantage of using this topology is that RSC has to be disabled and consequently, the generator consumers reac-

tive power leading to the deterioration of grid voltage [38]. To overcome this shortage, [38] has proposed a new converter protection which is primarily designed based on a Series Dynamic Resistor (SDR). This approach could help to avoid the DFIG control being disabled during fault condition. More details are given is Chapter 2.

1.1.1 Wind Energy in Australia

In 1994, wind energy was discovered to generate electricity and modern technology rapidly utilised in order to produce more power with high quality. Meanwhile, Australia has some of the best wind energy origins in comparison with other countries, mostly are located in Western, Southern-Western, Southern and Southern-Estern areas. However, the Australian government has pointed to reach up to 20% of all energy with employing renewable energies by 2020. According to [107] [108], the growing rate of wind energy in Australia has been over 40% per year since 2004.

Government policies, such as carbon emission reduction and Renewable Energy Target (RET) are the main influences in utilising wind energy resources in Australia.

Connecting wind energy is proven technology and has been in place for many years. Increasing in manufacture of wind turbines and competition between the manufactures, has led to a cost reduction of wind turbines [109].

However, there are some limiting factors in the development of wind energy such as the lack of electricity transmission infrastructure to access remote wind resources, and the intermittency and unpredictability of wind energy [110].

Growing Energy Demand in NSW

Table 1.1 details the capital expenditure over the 2009 to 2014 period for New South Wales (NSW) transmission and distribution companies.

This expansion has been justified because of the need to:

- Replace ageing assets
- Augment the networks to accommodate the growth in maximum demand for energy
- Improve network security and reliability

Table 1.1: Capital Expanditure between 2009/10 and 2013/14 for NSW Transmission and Distribution

	2009/10	2010/11	2011/12	2012/13	2013/14	Total
Trans Grid	523.3	447.1	549.7	505.2	379.7	2,405.1
Country Energy	715.7	757.5	776.5	779.1	797.2	3,826.0
Energy Australia's Distribution	1,132.7	1,281.7	1,422.2	1,377.1	1,423.3	6,637.7
Energy Australia's Transmission	263.7	174.2	245.3	320.4	197.0	1,200.5
Integral Energy	570.7	618.7	550.9	500.9	480.3	2,721.4

Growing Electricity Demand

Electricity demand is driven by economic activity, population growth, price, domestic air-conditioner penetration, the comparative cost of natural gas, and several less important factors. For residential growth, the key driver is population and hence household numbers. For commercial loads, the most significant drivers are economic activity and population growth. The electricity 10 year growth rate is estimated to be 1.5% per annum and projections for future growth are shown in Figure 1.1.

Figure 1.1: Energy Projections for Different Economic Growth Scenarios

The peak electricity rate continues to grow at a faster rate than the average growth rate. The summer peak 10% rate is forecast to be 2.2% and winter 2.0%.
Table 1.2 details the forecast growth in electricity demand and customer numbers over the 2009/10-2013/14 period for NSW distribution companies.

Growth Factor-Population

Electricity demand is directly related to population growth, and the growth varies significantly among NSW supply areas. Population growth in the supply area of Integral Energy is the highest in the state and its population is expected to grow by 6% by 2013/14, while the maximum demand for electricity is forecast to increase by 33% by 2013/14. Its supply area is served with rural and semi-rural feeders but is now becoming urbanised. This means that customers now expect improved reliability performance in these areas. In Country Energys supply area, population growth is pronounced only along the coastal strip and this population has a high penetration of air-conditioning. Meeting this peak demand growth is difficult by using non-network options, meaning that new infrastructure has to be built to service the loads.

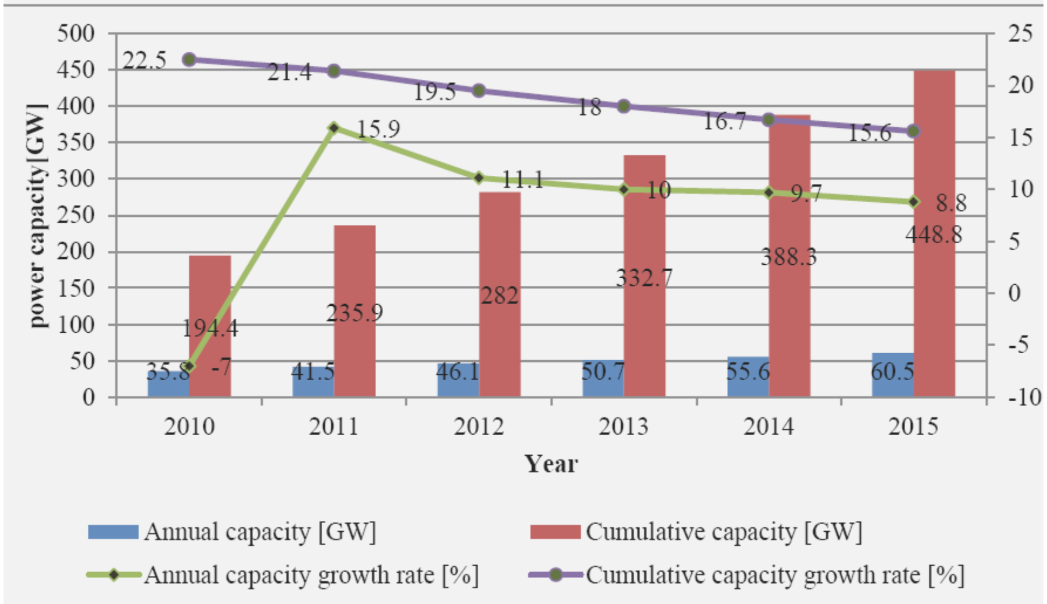

Figure 1.2: Forecasting Data from 2010 to 2015

1.2 Background

Wind power can contribute in saving the climate, as it could produce more than 12% of the electricity needed globally by 2020, saving 10 billion tons of CO_2 in the process, or 1.5 billion tons per year. The climate change program has to be seen as an economic and business opportunity at the same time as a driver to preserve the global environment. The forecasting data is shown in Figure 1.2 [111]

1.2.1 Overview of Wind Energy Conversion Systems

A wind energy conversion system is a system that converts the kinetic energy contained in the incoming air stream into electrical energy. This conversion occurs in two stages. The first stage occurs at the wind turbine blades which convert the kinetic energy stored in the wind into mechanical power. In the second stage, an electrical generator converts the harvested mechanical power into electricity.
A typical three blade Horizontal Axis Wind Turbine (HAWT) is shown in Figure 1.3 [111], [6], and its internal structure and major components are illustrated in Figure 1.4.

The advantages of the HAWT is listed as follows [7];

- Higher efficiency;
- Lower cost-to-power ratio;

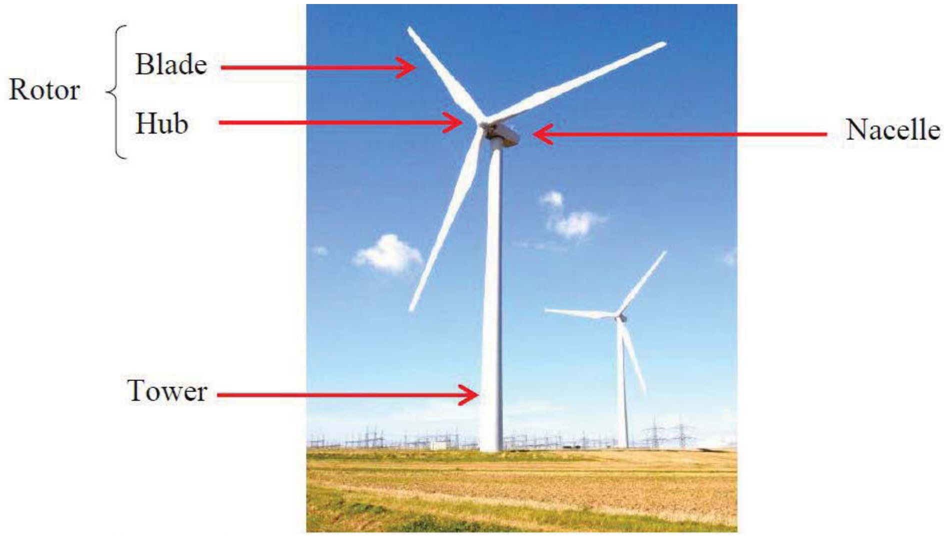

Figure 1.3: Utility-scale Horizontal Axis Wind Turbine
[111]

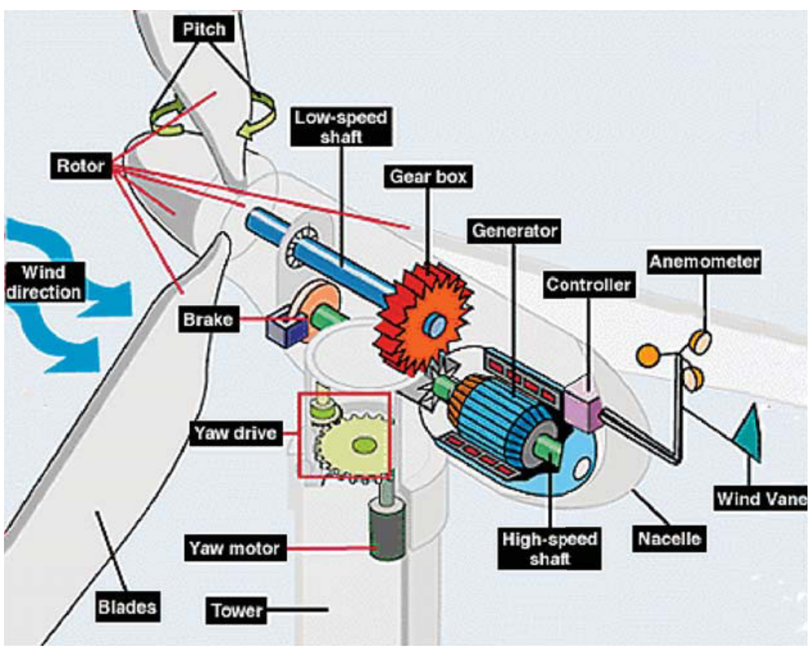

Figure 1.4: Internal Structure of HAWT

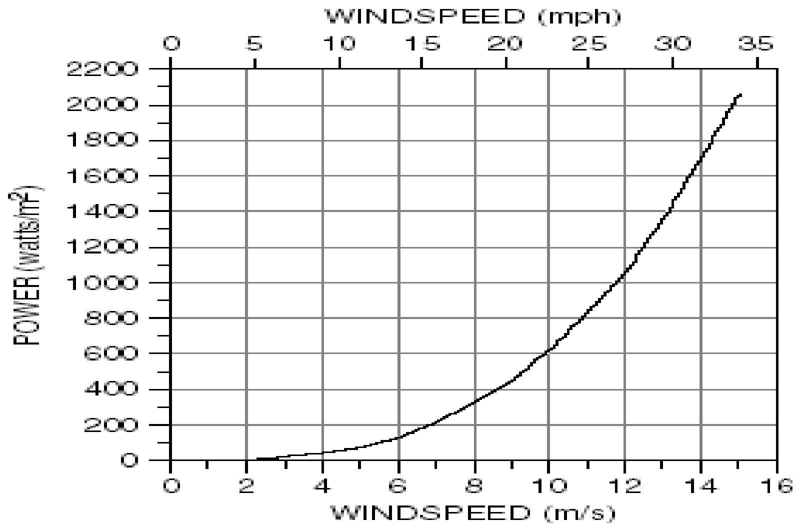

Figure 1.5: Power Curve of Wind Turbine

- Ability to turn the blades.

A HAWT has the following main components:

- Wind Turbine Rotor;
- Nacelle;;
- Tower;
- Yaw Mechanism.

1.2.2 Power in the Wind

Power of the wind is given by:

$$P_w = 0.5\rho A V^3, \tag{1.1}$$

where P_w is the power in wind (Watts), ρ is the air density (in $\frac{Kg}{m^3}$), A is the area of cross-section (in m^2), and v is the wind speed normal to A (in m^2). Figure 1.5 shows the power curve of the wind turbine.

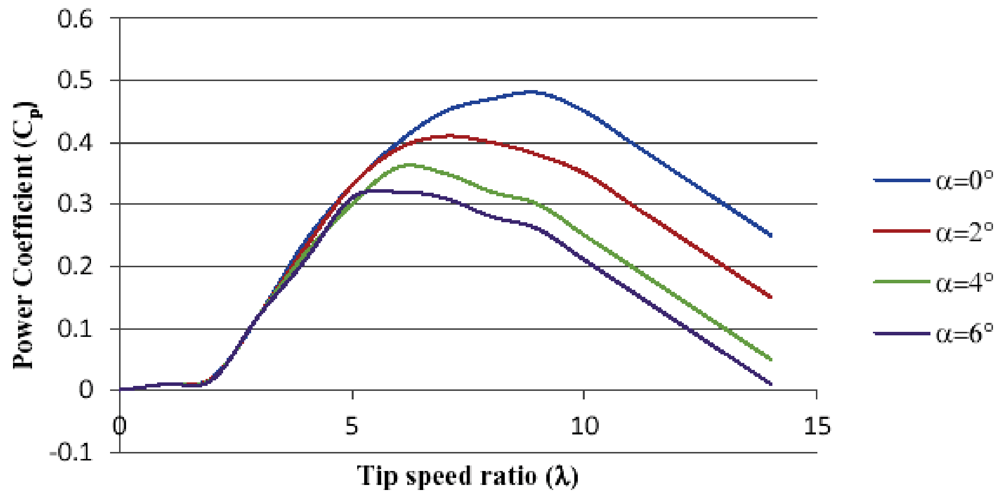

Figure 1.6: C_p versus λ curve

1.2.3 Power in the Turbine

The aerodynamic power in the rotor is given by [7]:

$$P_t = 0.5\rho A C_p V^3 \lambda, \tag{1.2}$$

where P_t is the power in turbine in (Watts), ρ is air density (in $\frac{Kg}{m^3}$), A is the area of cross-section (in m^2), V is the wind speed to A (in $\frac{m}{s}$), C_p is the power coefficient, and λ is the tip speed ration power coefficient.

1.2.4 Turbine Rotor Efficiency

Efficiency of the rotor is presented as a function of Tip Speed Ratio (TSR), the ratio between the rotational speed of a blade and the actual velocity of the wind. The TSR is calculated by:

$$TSR(\lambda) = \frac{w \times r}{V}, \tag{1.3}$$

where $w = 2\pi f$ is the angular velocity, v is the wind speed (in $\frac{m}{sec}$), and r is the rotor radius (in m).Figure 1.6 shows the C_p and λ curve for different values of the blade pitch angle α.

1.2.5 Power Extraction of Wind Turbine

Frequently, the wind turbine can work at maximum power point condition whereby this value can be calculated based on Maximum Power Point

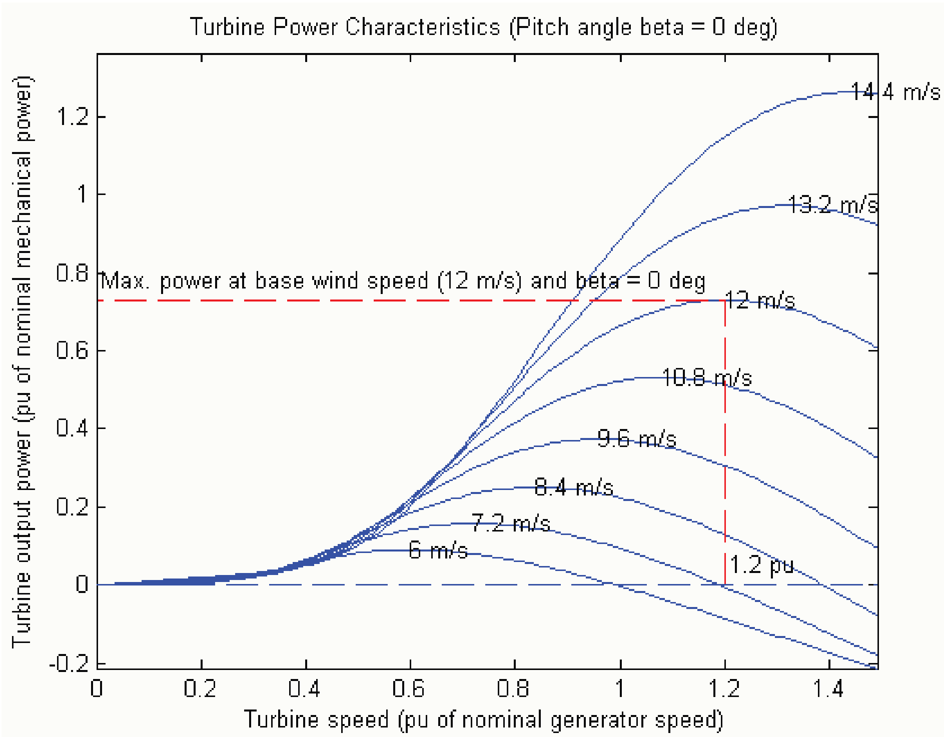

Figure 1.7: Maximum Power Point Tracking Determination Using TSR

Tracking (MPPT) techniques. Tip Speed Ratio (TSR) and Power Signal Feedback (PSF) control are the two main methods that have the ability to calculate the values of maximum power point. Figure 1.7 shows the details of various wind energy conversion system which are able to gain maximum power output.
The objective of PSF is to select the stored power curve by considering the rotor speed measurement so that gives the target optimum power which must be tracked by the system whereas the objective of TSR(λ) is to run the machine at the optimum λ by considering estimation of wind speed and rotor speed.

1.3 Wind Turbine Classification

Wind turbines can be operated in either variable speed or fixed speed mode.

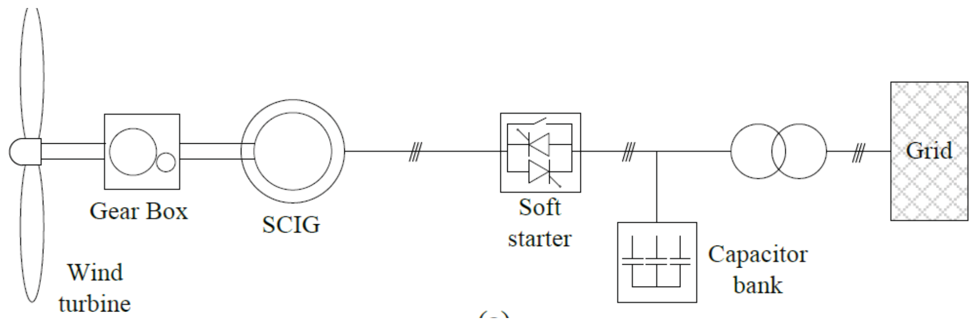

Figure 1.8: Conventional Fixed-Speed SCIG

1.3.1 Type A: Fixed-Speed

This formation characterizes the fixed speed controlled wind turbine. An synchronous squirrel cage induction generator (SCIG) is connected to the grid with a soft starter and a capacitor bank. The capacitor bank is applied to compensate the reactive power which is drawn by the SCIG. It provides the most robust system due to its simple configuration and a lack of converter. Note that this configuration is the cheapest; however, some drawbacks of this concept are as follows:

- It does not support speed control;
- It requires a stiff grid;
- Its mechanical construction must be able to support high mechanical stresses caused by wind gusts [8], [9].

1.3.2 Type B: Limited Variable Speed

Type B uses a Wound Rotor Induction Generator (WRIG). The generator connects to a transformer in series with a capacitor bank to compensate the reactive power. This generator has a rotor resistance which can be controlled by a converter installed on the rotor shaft. This helps to eliminate the requirement of expensive slip rings. Moreover, the output power and slip can be controlled by this control system [8], [9].

1.3.3 Type C: Variable Speed, Partially Scale Frequency Converter

This type of generator is known as the Doubly-Fed Induction Generator (DFIG) and applies to variable speed wind turbines with WRIG and fre-

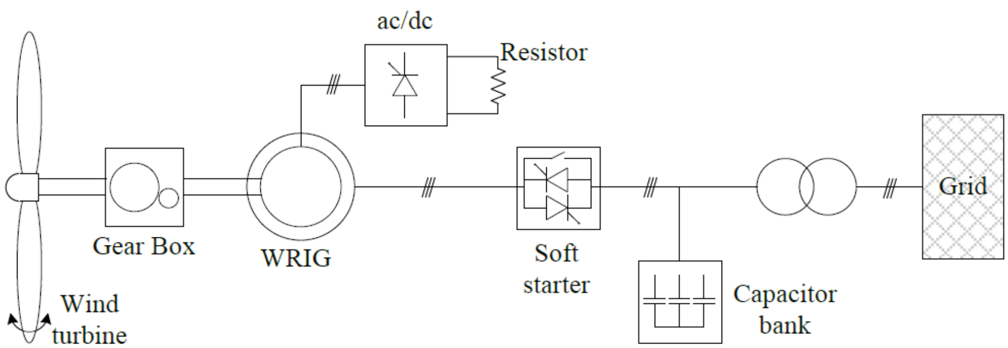

Figure 1.9: WRIG with Variable External Rotor Resistance

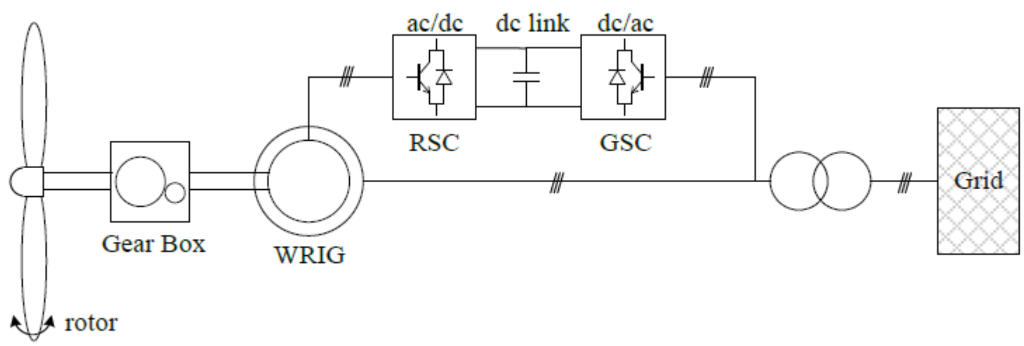

Figure 1.10: DFIG Grid Connected Concept

quency converter on the rotor side of the circuit. The stator is directly connected to the grid side. The aim of this type of generator is to compensate reactive power. This converter can have a speed range up to 30-40% of that of a synchronous generator [8].

1.3.4 Type D: Variable Speed; Full Scale Frequency Converter

This is a full variable speed wind turbine with WRSG, PMSG or SCIG connected to the grid via a full scale frequency converter. The concepts of full frequency converter are its ability to reactive power compensation and to help smooth the grid connection. They use a direct driven mulitiple generator with a large diameter instead of a gearbox which is an advantage of some full variable speed wind turbine systems [9].

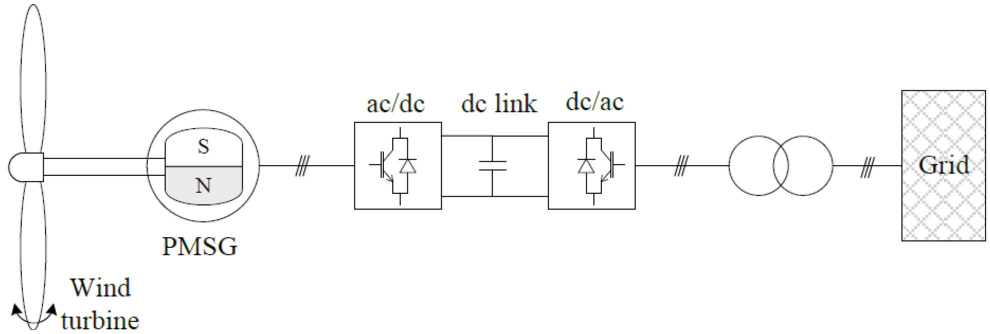

Figure 1.11: PMSG with Full Scale Converter

1.4 Thesis Outline

The outlines of this thesis is organised as follows:

Chapter 2 presents a literature review on the grid code requirements, low voltage ride through (LVRT), fault ride through (FRT) and Dubly Fed Induction Generator (DFIG). It also provides the DFIG theories and describes different types of power converters and its protection system.

Chapter 3 details the dynamic wind energy conversion system (WECS) model besides modelling of different WECS subsystems; drive train, aerodynamic and electrical subsystems. The behaviour of the DFIG-based wind turibne is studied under different modes.

Chapter 4 presents the concepts of voltage instability and driving force. It also analysed the main causes of voltage instability. Different levels of DFIG-based wind turbine control are given.

Chapter 5 first presents an overview of Model Predictive Control (MPC) techniques. Then, a multi variable control strategy is introduced for all operation regions of the DFIG-based wind turbine.

Chapter 6 summarizes the thesis contributions and offers suggestions for further improvements.

Table 1.2: Distributor's Customer Numbers and Energy Forecasts for 2009/14

Forecast	2009/10	2010/11	2011/12	2012/13	2013/14	Ave. Annual
Country Energy's Customers (No.)	1,321,286	1,339,074	1,357,118	1,375,421	1,393,989	1.3%
Energy Australia's Customers (No.)	2,073,691	2,087,691	2,102,703	2,117,640	2,132,584	0.6%
Integral Energy's Customers (No.)	860,392	866,018	873,565	885,078	896,496	1%
Country Energy's Energy Forecast (GWh)	12,092	12,147	12,202	12,556	12,314	0.5%
Energy Australia's Energy Forecast (GWh)	27,948	28,041	27,989	27,673	27,477	-0.1%
Integral Energy's Energy Forecast (GWh)	17,373	17,313	17,526	17,967	18,202	0.7%

Chapter 2

Wind Turbines with Doubly-Fed Induction Generators

2.1 Introduction

With modern technology, Doubly-Fed Induction Generators (DFIGs) are frequently used in order to produce electricity in large wind turbine because of their outstanding advantages over other types of generators. The main advantage of using such generators for wind turbine is their ability to maintain amplitude and frequency of output voltage at desired constant rates irrespective of the wind speed. Moreover, the DFIG can be connected directly to an AC power network besides generating electrical power at lower speeds [10, 11].

In recent years, DFIG trends to high penetration of wind power that has commanded to provide Low Voltage Ride Through (LVRT) capability.

However, DFIGs require complex power conversion compared with asynchronous machine. Although synchronous generators have the same advantages as DFIG, but the AC-DC/DC-AC converters in a DFIG have smaller output power. This is because of their converter ability which acquires 30% of the nominal generator output power for DFIGs [8, 9].

2.1.1 Advantages of VSVP Wind Turbines

Because of their flexibility to control [12], types C and D are the most commonly used in power systems known as Variable Speed Variable Pitch wind turbines. The main advantages of these types of wind turbines over types A and B are listed below [13–16]

- Because of their ability to adjust turbine speed continuously in order to track all wind speed variations. It is important to keep the power coefficient at the maximum value in the partial load regime.

- Variable speed wind turbines help to reduce the drive train torque fluctuation which can absorb kinetic energy as the variations in the wind speed. Moreover, Types C and D can create elasticity which can help to relieve the loads affecting the wind turbine.

- Variable speed wind turbines allow delivering smooth power into the grid. The fluctuating wind turbine speed, inertia of the system acts as an energy buffer between the input power and the power delivered to the grid. In the case of high wind speed, the increased input power can be stored as kinetic energy in the turbine. The process will be reversed in the case of low wind speed.

- The use of variable speed wind turbines allows reactive power control to deliver smooth wind turbine power with less voltage fluctuation and better power quality. However, fixed-speed wind turbines do not have this ability to generate reactive power in order to support the grid voltage.

2.2 Wind Turbine Control

The most important objective of wind turbine control is to maximize the captured energy. Figure 2.1 shows the operation of wind energy conversion system at its maximum power coefficient, $C_{p,max}$. The following conditions must be satisfied.

- The pitch angle should be fixed at its optimal value β_0 (typically very close to 0).

- The tip speed ratio should be fixed at its optimal value λ_0(typically between 6 and 8 for three-bladed HAWT [6]). This is achieved by continuously varying the turbine speed w_t to match variations in the wind speed such that the ratio $\frac{w_t R}{V}$ is kept constant at λ_0.

Fixed-speed wind energy conversion systems can operate at maximum efficiency for only one value of the wind speed, whereas variable speed wind conversion system can work over a range of wind speeds.
When the wind turbine is operating at $\lambda = \lambda_0$, $\beta = \beta_0$, and consequently

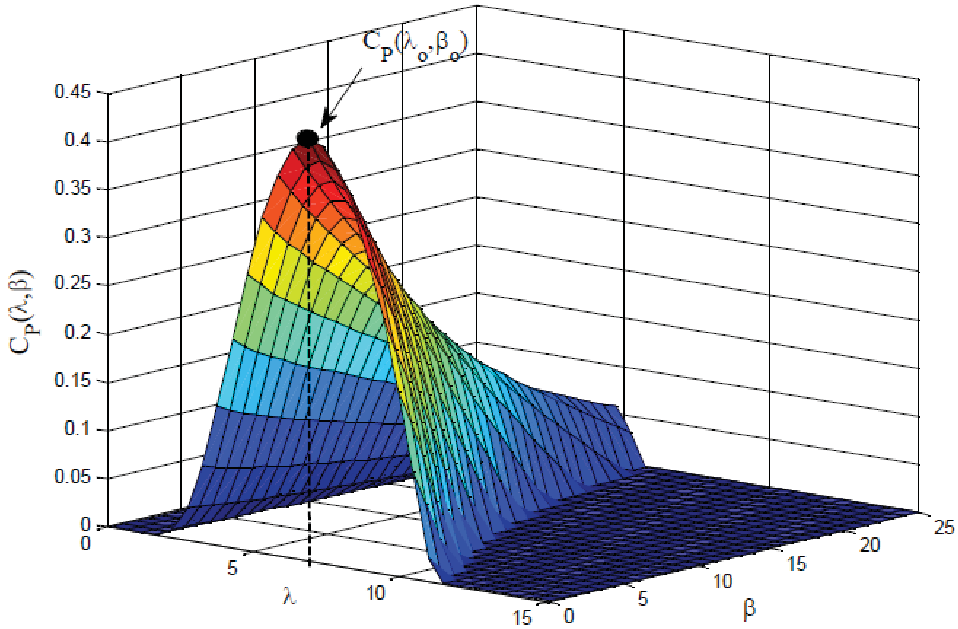

Figure 2.1: Typical Power Coefficient Variations at HAWT

$C_p = C_{p,max}$, the wind turbine is said to be working at the Optimal Regime Characteristic (ORC) [5, 17]. At the ORC, the turbine power and torque are given by (2.1) and (2.2), respectively, where k_0 is defined in (2.3). Figure 2.2 shows the ORC in the $P_t - w_t$ and $T_t - w_t$ planes.

$$P_{t,ORC} = k_0 w_t^3 \tag{2.1}$$

$$T_{t,ORC} = k_0 w_t^2 \tag{2.2}$$

$$k_0 = \frac{1}{2\lambda_0^3} C_{p,max} \rho \pi R^5 \tag{2.3}$$

2.2.1 Limiting the Power of a WECS

As seen in Figure 2.3, when the wind speed is higher than v_{rat}, the power taken from the wind limits of the wind turbine components. Hence, the aerodynamic power must be limited to the rated value by reducing the rotor efficiency, which can be realized by controlling angle of attack.

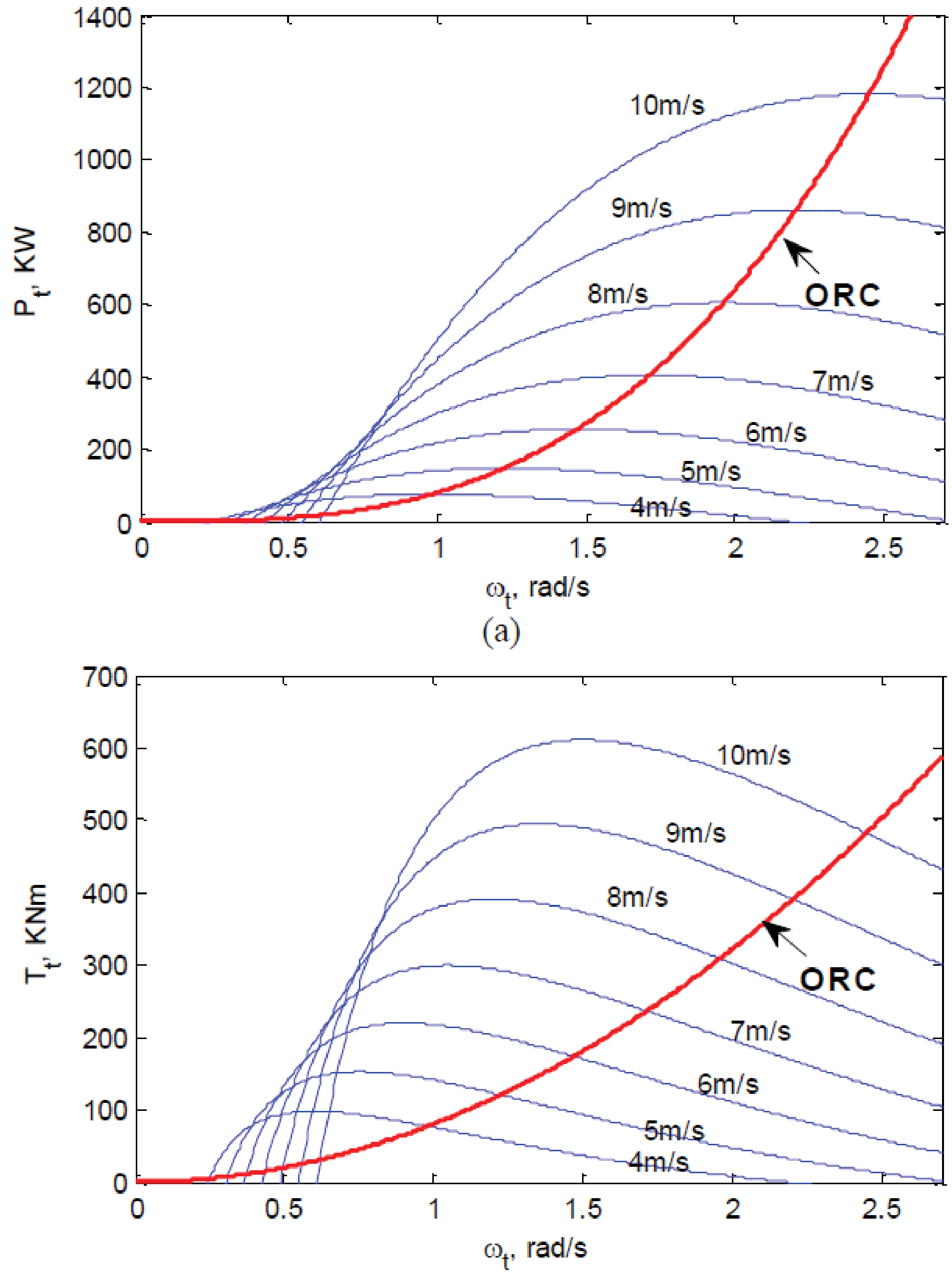

Figure 2.2: ORC, Wind Turbine Power, and Torque Curves at Different Wind Speeds at $\beta = 0$

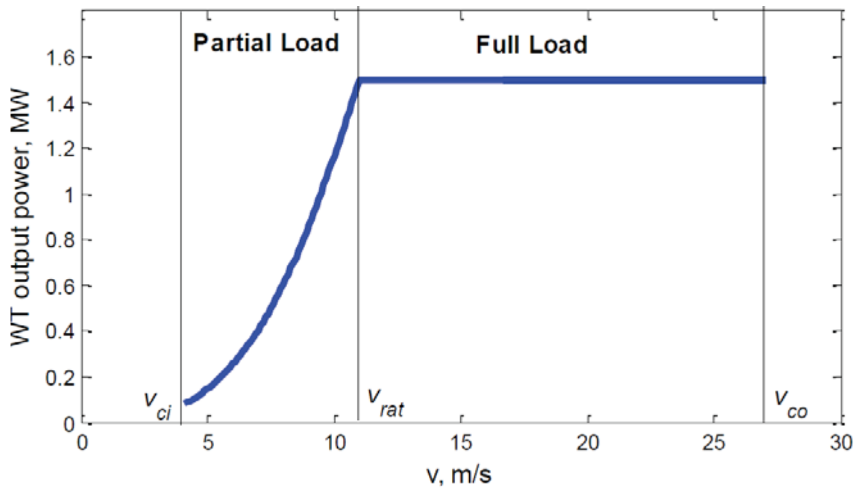

Figure 2.3: Output Power Curve of a 1.5 MW Wind Turbine in Partial Load Regime and Full Load Regime

2.3 Control Modes

Figure 2.3 depicts regimes with two different control objectives in a variable speed variable pitch wind turbine.

The partial load regime includes all wind speeds, v, which ranges between v_{ci} and rated wind speed, v_{rat}. In this part, wind speed has low values and the captured power is less than the rated wind turbine power. Thus, the objective control in this regime is to maximize the energy capture by varying the turbine rotational speed and fixing the blades pitch angle at its optimum value.

The full load regime normally happens if the wind speed is above v_{rat} and below the cut-out wind speed v_{co}. In this case, the available wind power is higher than the rated wind turbine power. The control objective of this regime is to regulate the wind turbines output power at the rated value by adjusting the pitch angle of the blades.

In the case of wind speed is less than $5\frac{m}{s}$ or more than $25\frac{m}{s}$, the wind turbine is shut down. The reason goes back to available wind power, which is much smaller than the wind turbines operational losses and much higher than the wind turbines design limits, respectively.

2.3.1 Control Challenges

Maximizing the cost-effectiveness of wind power generation is the main objective of wind turbines control [5, 18]. Besides that, we also have the following objectives:

- Maximizing the energy captured;
- Reducing mechanical loads, especially those resulting from drive train torque pulsations causing costly gearbox failures;
- Reducing the wind turbines down-time by increasing the system robustness against changes in wind turbine dynamics, which result from faults, wear, debris buildup on the blades, etc;
- Enhancing the power quality by smoothing the output power and reducing voltage fluctuations at the point of interconnection to the grid;
- Ensuring compliance with recent grid codes and providing grid support during severe network disturbances such as short circuits.

Realization of all above-mentioned objectives is not an easy, particularly when high fluctuation appears in power system. Moreover, considering the system nonlinearity, the physical constraints and the multi-input-multi-output (MIMO) nature of the system make the control design problems even more challenging. The difficulties of control design are associated with details of generator and wind turbine control levels.

2.3.2 Wind Turbine Control Level

The first control challenge in partial load regime is maximizing the conversion efficiency while minimizing the dynamic loads. As mentioned in [17, 19–21], large generator torque variations, severe frazzle loading and high mechanical stresses are the main causes of wind turbines turbulence. They can damage the wind turbine components and consequently costly failures. The control system has to be designed to achieve a reasonable balance between load minimization and energy maximization.

On the other hand, speed and output power regulation is the main control task in full load regime, especially in the event of severe fluctuations normally caused by uncertain variations in wind speed. Therefore, this variation affects both wind energy conversion system life time and power quality.

Transition regime is defined when the wind turbine operates at wind speeds around the rated value. In this regime, full load and partial load wind turbines controllers have to be switched continuously. This switching can cause power overshoots and undesirable transient loads [18]. The work of [22]has stated that the maximum mechanical damage happens during this transition.

[17, 20, 23–29] have proposed many control techniques to control wind energy conversion systems in the partial load regime. The standard Proportional Integral (PI) controllers is described in [17,18,20,23,24]. On the other hand, [17] has proposed the use of Linear Quadratic Gaussian (LQG) controller to trade-off between maximizing output power and minimizing load reduction and also to deal with system nonlinearity besides [18], [25]which has proposed use of a gain scheduled controller. Moreover, [26, 27, 29] have applied sliding mode control and feedback-linearization to handle nonlinearities. In [28], adaptive control methods are proposed to design the wind turbine controllers.

In the full load regime, recently, many researchs have focused on control of variable-speed-variable-pitch wind turbines [20,30–32]. However, [20,31,32] have ignored the multivariable nature problem. At typical PI controller is applied in an adaptive self-tuning and power control loop in [31]. [30] has applied a gain scheduled H_∞ controller, while a state feedback controller is designed in [32].

Decentralized methods are developed to control the speed and wind turbine power independently. The reported works have defined for the full load or partial load regime. [18], [30] have established that a high performance of the power system can be achieved by considering the multivariable nature problem and applying a MIMO controller. [18], [33] propose a multivariable controller and gain scheduled H_∞ controller, which can work in both full load and partial load regimes. To the end, however, no control method is available to eliminate the power and torque overshoots in the transition region.

2.3.3 Generator Control Level

In modern wind turbines, while it is not required to control just the active and reactive power generation over the providing high performance control, it should meet other requirements that enforce by grid codes. One of the most important of these requirements is the Fault Ride Through (FRT) or Low Voltage Ride Through (LVRT) capability [34–38]. This requirement identifies the expected behaviour of wind turbine during and right after the grid faults to achieve a good performance while guaranteeing stability of the power network stability.

A critical problem for DFIG-based wind turbine is the large voltage dip,

which typically happens when an external grid fault occurs. This problem occurs at wind energy conversion system terminals, resulting in overcurrent or overvoltage in the power converters and generators. DFIG-based wind turbines are more sensitive to high current because of rated power converter which is 30% of the generator power. Voltage dips can lead to the converter destruction unless protective actions are employed [39–41].
One of the most common protective methods is crowbar protection that disables the rotor side converter of the DFIG-based wind turbine. A crowbar protection acts to induce the high rotor currents into a resistive circuit. After fault clearance, the crowbar is disconnected and the rotor side converter is reactivated and the DFIG continues its normal operation. New grid code requirements, this approach is rejected. Here, a wind turbine must remain connected during grid faults to be capable to compensate the required reactive power [45]. The drawback of using crowbar protection is the loss of controllability of DFIGs once the RSC is disabled. During this period, DFIGs act as a consumer of reactive power which leads to deteriorate the voltage recovery of the system.
Recently, many researchers have focused on finding a solution that improve FRT or LVRT capability for DFIGs with new protection and control strategies [35–38,43–48]. [49] has proposed a conventional PI controller to modify the RSC control algorithm. These algorithms improve the FRT capability without using hardware protection. Rotor side converter control was proposed in [43] based on stator flux demagnetization. Moreover, a fuzzy logic controller is proposed to control the current of rotor in [44]. [45] has used additional feed-forward compensation to control the rotor current. Although all above-mentioned strategies could successfully improve the FRT capability, they can only do so in a small magnitude of voltage dips [40]. It has been shown that fault ride through cannot be solved simply by DFIG control in the case of severe voltage dips.
As mentioned before, this shortage has motivated other researches to discover new protection strategies instead of using traditional crowbar protections e.g. [36–38, 48]. The advantage of these methods is because of their ability to preserve DFIG over DFIG rotor during severe voltage dips. Another proposed solution for FRT difficulty is installation of static synchronous compensator (STATCOM) at the wind farm which was firstly proposed in [46, 47]. The goal of adding such an expensive component STATCOM is to provide supporting reactive power during grid faults.

2.4 Grid Faults and Requirements

Network voltage is responsible for most of the events in the electrical network. The events can be changed from milliseconds to hours by different magnitude. Network events faults can be categorised according to the duration of the faults and the voltage magnitude. A typical fault is when the wind turbines are connected to the grids which are subjected to grid faults. The faults or electrical network events are defined as an error from nominal operation conditions. Normally, the deviation happens because of earth faults, operating large motors or adding large loads and short circuits in the grid, leading to under voltage or voltage sag [50, 51].

2.4.1 Grid Requirements

In the early days, the main goal was to keep the wind turbines disconnected in the event of disturbance. As such, grid code was applied to generators to protect wind turbines and network distribution and to prevent degrading the system performance. Because of the integration of large scale wind turbines, wind energy became a major contributor to electricity generation. However, a robust performance of wind turbines during faulty period deemed necessary. One of the most important requirements of the grid code is Low Voltage Ride Through (LVRT) capability to improve the transient stability of power system and the reactive power capability to satisfy the voltage requirements of power systems. Consequently, every wind turbine generator needs to have voltage ride through capability.

Wind power has a large impact on the power grid stability on power system operation which caused to increase the connection requirements which came out with different grid codes. Generally, wind turbines must organize the same operation behaviours as the conventional generation and responsibility for the network system to let grid codes cover a wide range of voltage level. However, wind power must support frequency and voltage of the grid besides capability to regulate active and reactive power.

Moreover, grid requirements have focused on low voltage ride through capability during disturbance and system fault, quality, active and reactive power control [50]. The main issues for the grid connection are [52]:

- Voltage operating range;
- Frequency operating range;
- Active power control;
- Frequency control;

- Voltage control;
- Reactive power control;
- Low voltage ride through (LVRT);
- High voltage ride through (HVRT);
- Power quality;
- Wind farm modelling and verification;
- Communications and external control.

These items can be classified under three main requirements: low voltage ride through and power plant modelling, frequency and voltage control; and quality and power control.

2.4.2 Power Control Quality Capability

Wind turbine power has to support reactive and active power for the grid according to the grid power requirements. In addition, wind turbines also have to share their duties such as required load for short and long period. The delivered power must have good quality with acceptable range of current and voltage [50].

2.4.3 Frequency Control Capability

Wind turbines that are unified with power network system have to control with frequency requirements allocated by the conventional power system. Wind turbines must have this capability to work within typical frequency variation range. For example, grid codes in the UK needs that wind turbines to work between 47.5 Hz and 52 Hz continuously and at least 20 seconds between 47 Hz and 47.5 Hz. Furthermore, working with a large frequency deviation over these limits may lead to capacity loss and black-out [52, 53].

2.4.4 Voltage and Low Voltage Ride Through Capability

Wind turbine power plants must have the capabilities to work with the required grid voltage variation. They have to produce the same voltage with the required conventional power system to keep that voltage constant [52]. Voltage ride through is requested for wind turbine in order to avoid the produced power during grid faults. Due to a rapid increase of wind power generation, low voltage ride through helps such systems to avoid some voltage and frequency control which might happened because of disconnection of wind turbines. The purpose of voltage ride through is to keep the wind turbines remain connected to the grid during faults and to support the reactive power in compensating the required voltage [50]. However, with fast development of wind power plants, voltage support is becoming standard for all grid codes such as three phase, single and two phase faults [20, 52].

2.4.5 Power Plant Modelling and Verification

As it mentioned before, the power plants must be modelled and controlled to meet the connection requirements. Simulation tools can be used to simulate and control the power plant and keep the voltage within the allowed voltage fluctuation limit. Moreover, high power quality is needed to be approved with simulation tools in acceptable current and voltage harmonics [20, 26].

2.5 Low Voltage Ride Through (LVRT) Different in Grid Codes

Modern wind turbines play an important role in grid utilities which are usually assembled in a large scale. Previously, there was no major effect on the utility grid because of low penetration of wind power. At that time, the generators could be disconnected from the grid during faults which led to the loss of power generation. However, it was not assumed as a threat to the overall system. Later, as size of wind farms increases, the impact of power losses could be severe when the whole wind farms are disconnected due to the faults. Therefore, a new grid code has been introduced the Low Voltage Ride Through (LVRT) or Fault Ride Through (FRT) capability. LVRT or FRT means that the new wind turbines must have the ability to keep their connection during faults and any kinds of disturbances. The LVRT requires the generators to keep the frequency and voltage of the system stable by injecting active and reactive power to the grid. Figure 2.4 shows the behaviour of the wind turbine during fault based on LVRT curve. The LVRT curve can be divided into four areas as below:

- Area 1 The fault has to be clear at t_{min} and voltage dip must not reach lower than V_{min}, and the wind generator must stay connected.

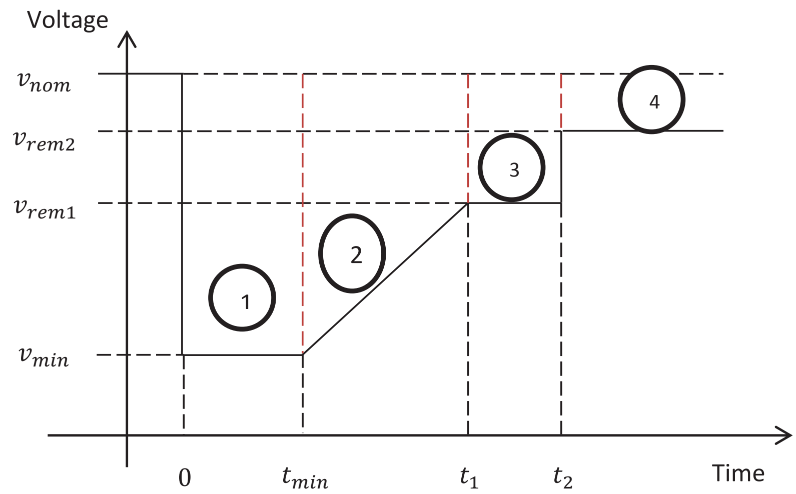

Figure 2.4: Low Voltage Ride Through Curve

- Area-2 The voltage recovery occurs from V_{min} to V_{rem1} in the time period $[t_{min}, t_1]$.
- Area-3 The voltage recovery continues before it reaches Area-4.
- Area-4 The nominal operating voltage occurs.

To summarize the LVRT curve, the system must be disconnected if the voltage beyonds the grey area. However, the boundary limits will be different depending on the regions or countries. During a fault event, the wind generator must provide reactive power to the grid as required to keep the power system stable. In simulating this LVRT, the system runs normally for 0.5 seconds . Then, the fault event last for 1.15 seconds before getting cleared [54].

2.6 Reactive Power Capability

Mostly, the new large scale wind turbines are equipped with Doubly-Fed Induction Generators (DFIGs). With a rapid increasing level of wind power penetration into the grid, DFIGs have generated a widespread concern regarding its impact on power system performance. Another factor which is important to plant operation is the power factor at Point Common Coupling (PCC) so that remain between 0.95-0.9 [55]. The reason for this bound refers to the reactive power capability for a wind plant which is major additional cost compared to conventional units. As before, another significant focus of grid codes is on the active and reactive power control capability in order to control frequency and voltage in the grid, respectively [56].

Stable operation of power system requires the availability of enough reactive power generation so that reactive power plays an important role in stability of power system. Moreover, dynamic and static reactive power sources are essential in voltage controllability. However, a DFIG being the most principal wind generator assembled in modern wind farms because of their high impacts on the current power system control and stability. Consequently, it is important to analze the reactive power capability of the DFIG.

2.7 Reactive Power Capability Limitations with DFIG

To specify the reactive power limits in DFIG, the specification of power converter and the electromechanical features of the generators must be taken into consideration. Although DFIG can control reactive and active power independently the capability of reactive power for those generators also depends on the limitation of the rotor voltage, stator and rotor current and the slip [57, 58]. The stator voltage is assumed constant because it is influenced by the wind turbine design which is given by the grid. The required rotor voltage is directly proportional to the slip; therefore, determining the limitation of rotor voltage is essential for the rotor speed interval. It is concluded that the rotor speed is limited by the rotor voltage limitation. Lastly, the stator current is another effective parameter and its limitation depends on the generator design, whereas the rotor current and rotor voltage limits depend on both power converter and generator design.

2.8 Power Converters

Figure 2.5 depicts the AC/DC/AC bidirectional power converter in DFIG which is connected back-to-back the rotor circuit and the grid. In order to minimize the output of grid side, a RL filter is used in grid.

2.8.1 Rotor Side Converter

The aim of Rotor Side Converter (RSC) is to control the active power by determining a torque reference which is delivered by DFIG. The reference for reactive power is normally determined by a PI controller to measure the grid voltage and compare it with a reference. Reactive power capability and

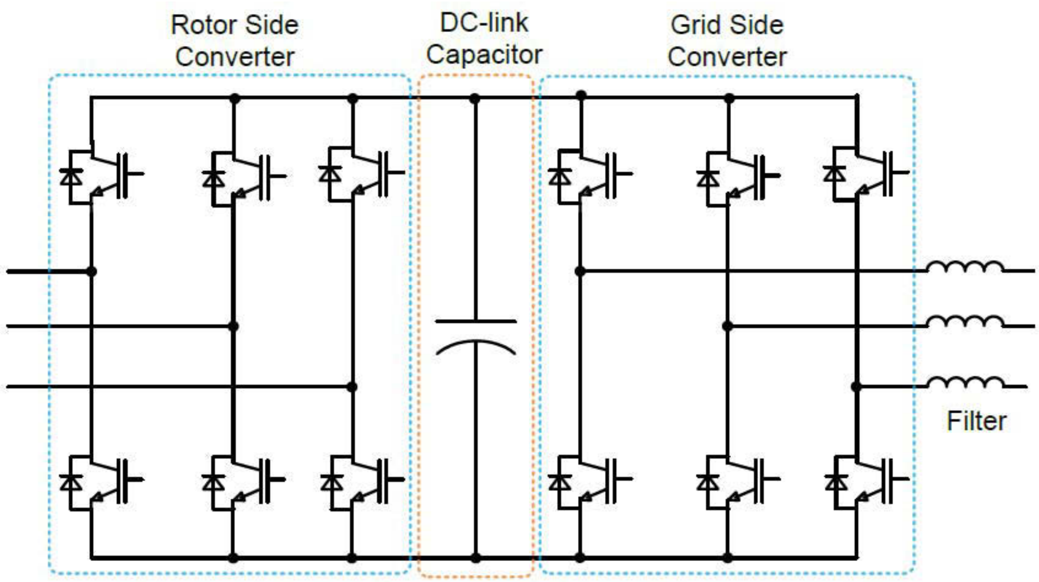

Figure 2.5: The ac/dc/ac Bidirectional Power Converter in DFIG

maximum slip power are the two factors that determine the power rating of RSC. However, the objective of RSC controller is to regulate the rotor speed or stator side power and stator side reactive power independently. Figure 2.6 depicts the block diagram of the RSC control design.

2.8.2 Grid Side Converter

The control objective of Grid-Side-Converter (GSC) is to keep the DC-Link capacitor voltage at a desired level while not contributing to reactive power injection ($I_q = 0$). It is essential to find a solution for this limitation since we know the reactive power injection through the GSC is useful to improve LVRT capability in a faster voltage recovery. Moreover, the GSC can be operated to support grid reactive power during faults so that enhance gird power quality [59, 60].
The amount of energy stored in the dc-link capacitor is written as:

$$E_c = \int P dt = \frac{1}{2} C V_{DC}^2, \tag{2.4}$$

where P is the net power flow into the capacitor, C is the DC-link capacitor value and V_{DC} is the capacitor voltage. P is equal to $P_r - P_g$, where P_r is the rotor power inflow and P_g is the grid power outflow.

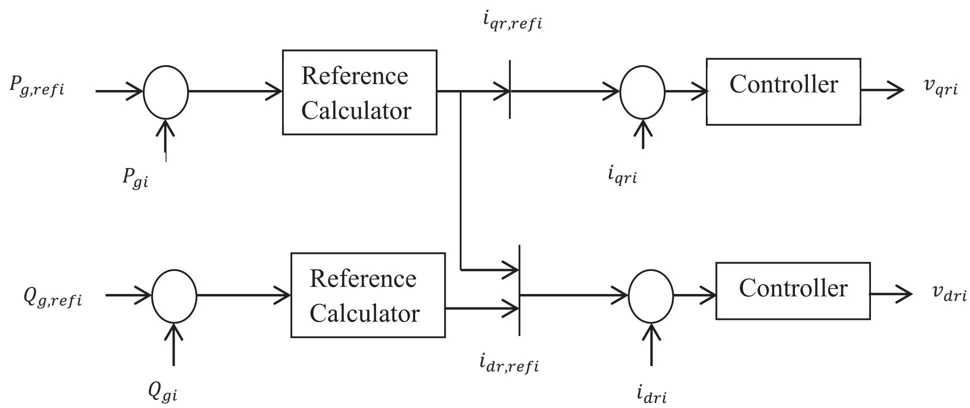

Figure 2.6: Schematic Block Diagram of Rotor Side Converter Control

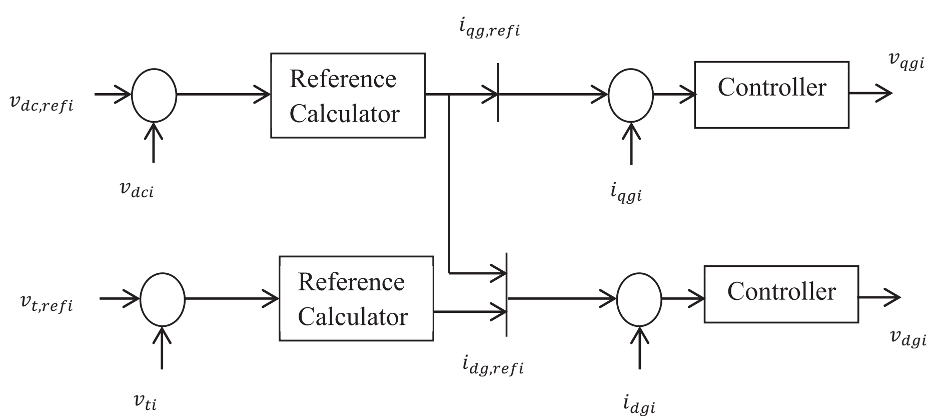

Figure 2.7: Schematic Block Diagram of Grid Side Converter Control

2.9 Converter Losses

The main causes of rotor side converter and grid side converter losses refer to switching and conducting losses caused by the off-on turning in transistors and current of transistors or diodes, respectively. Short circuiting of rotor winding occurs when the protection devices such as crowbar detect overvoltage or overcurrent. In this case, it is essential to remove this short as fast as possible to maintain a nonstop operation. In this way, it is feasible to make reactive current compensation to help recovery from the fault [61].

2.10 Converter Protection Schemes for DFIG

The converter system consists of a set of resistors connected to the rotor winding in to prevent implicit diturbances. The crowbar protection bypasses the rotor side converter when the fault occurs. In addition, a DC chopper can also be connected to DC-Link capacitor in parallel to control the limit of the overload when the grid has a low voltage. Other protection methods used in fully rated converter topologies.

2.10.1 Crowbar Protection

Most commonly used in DFIG protection, the crowbar protection consists of a set of resistors connected in parallel with the rotor to bypass the rotor side converter. The crowbar resistance is connected when necessary and is then disabled to continue DFIG control.
Current and voltage of RSC are critical references for regulation. Their limits must not be exceeded. To do that, control signals will be activated from the RSC components while are typically Insulated Gate Bipolar Transistors (IGBT), whereby DC-Link voltage can change quickly under the desired conditions to trigger the crowbar. Moreover, IGBTs and Gate Turn-Off Thyristors (GTO) and Bidirectional Thyristors are after used for switching [62–65].

2.10.2 DC-Chopper

Another DFIG protection device is the braking resistor or dc-chopper [63, 66], which is also connected in parallel with a DC-link capacitor. The Dc-chopper limits overcharging during a low grid voltage. Therefore, it can protect IGBTs from overvoltage while not affecting the rotor current.

Moreover, dc-chopper can be installed as a protector of DC-link capacitor in a full rated converter [67].

2.10.3 Series Dynamic Resistor (SDR)

Series Dynamic Resistor (SDR) is located in series with the rotor and act as a switch to limit the rotor overcurrent. It is ON during the normal operation, meaning that the resistors are bypassed. It is OFF during fault conditions, meaning that the resistors are connected to the rotor winding. The big advantage of SDR over the crowbar and dc-chopper is because of its ability to suffer high voltage, while it can be shared between resistors. Furthermore, the shared high voltage does not lead to a loss of converter control. On the other hand, SDR can be used to control the rotor overvoltage and limit the high rotor current.

Another advantage of using SDR is that the rotor side converter does not require to be inhibited during the grid fault because the limited current leads to reduce the charging current of DC-link capacitor so that avoid dc-link overvoltage as well.

Chapter 3

Model of Wind Turbine Devices based on DFIG

3.1 Dynamic Model of Wind Generators

Dynamic modeling of DFIG-based WT is discussed in [68]. This reference compares the 5^{th} and 3^{rd} order models used for the DFIG machine. The 5^{th} order model comprises the electrical dynamics of stator and rotor, as well as a single-mass drive train model for mechanical dynamics. The 3^{rd} order model neglects the stator dynamics. To analyze the dynamic behaviors of DFIG-based WT under grid disturbances and wind speed fluctuations, a more detailed model is required. In addition to the stator and rotor dynamics, this model should include a multi-mass representation of the drive train, the rotor dq controllers and speed/reactive power controllers, as follows;
The generalized machine model is developed based on the following conditions and assumptions:

- A Positive direction for the stator and rotor currents is assumed into the generator;

- All system parameters and variables are in per unint and referred to the rotor side of the DFIG.

This thesis uses a model of the induction generator written in appropriate d-q reference frame to facilitate the investigation of control strategies. Figure 3.1 depicts the general structure of the model of a constant-speed wind turbine. The most important components of a constant speed wind turbine are rotor, drive train and the generator.

3.2 Rotor Model

WTs are the main components of wind farms. They are usually mounted on towers to capture the most kinetic energy. Because the wind speed increases with height, taller towers enable turbines to capture more energy and generate more electricity. The three bladed rotor, consisting of the blades and a hub, is the most important and most visible part of a WT. It is through the rotor that the energy of the wind is transformed into mechanical energy that turns the main shaft of a WT.

$$T_{ae_i} = \frac{\rho_i}{2} A_{wt_i} c_{p_i}(\lambda_i, \theta_i) V_{w_i}^3, \tag{3.1}$$

where c_{p_i} is approximated by the following relation:

$$c_{p_i} = (0.44 - 0.0167\theta_i)\sin[\frac{\pi(\lambda_i - 3)}{15 - 0.3\theta_i}] - 0.00184(\lambda_i - 3)\theta_i, \tag{3.2}$$

for $i = 1, 2, \cdots, n$, where n is the total number of generators, T_{wt_i} is the aerodynamic torque applied to rotor for the i^{th} turbine by the effective wind speed passing through the rotor, ρ_i is the air density (kg/m^3), c_{p_i} is the performance coefficient or power coefficient, $\lambda = \frac{w_{m_i} R_i}{V_{w_i}}$ is the tip speed ratio, R_i is the wind turbine radius (m), w_{m_i} is the rotor shaft speed (m/s), θ_i is the pitch angle (degree), and A_{wt_i} is the area covered by the wind turbine rotor (m^2).

A two-mass drive train model of a wind turbine generator system (WTGS) is used in this study as the drive train model can satisfactorily reproduce the dynamic characteristics of WTGS.

The dynamics of the shaft are represented as $i = 1, 2, \cdots, n$. A controller equipped with a WT starts up the machine at wind speeds from 8 to 16 miles per hour (mph) and shuts it off at about 55 mph. Turbines do not operate at wind speeds above about 55 mph because they might be damaged. The radius of a 2 MW wind turbine is about 80m. The typical value of air density is 1.225 kg/m3. cp is in the range of 0.52 - 0.55. The towers range from 60 to 90 metres (200 to 300 feet), and the blades rotate at 10 - 22 revolutions per minute.

3.3 Shaft Model

A two-mass drive train model of a WT generator system (WTGS) is used in this thesis. Drive train modelling can satisfactorily reproduce the dynamic characteristics of a WTGS since the low-speed shaft of a WT is relatively soft [69]. Although it is essential to incorporate a shaft representation into the constant-speed wind turbine model, we only include a low-speed shaft. The gearboxes and high-speed shafts are assumed to be infinitely stiff. The resonance frequencies associated with gearboxes and high-speed shafts usually lie outside the frequency bandwidth of interest [70]. Therefore, we use a two-mass representation of the drive train as follows:

$$\dot{w}_{G_i} = \frac{K_{s_i}\gamma_i - T_{e_i} - D_{G_i} w_{G_i}}{2H_{G_i}}, \tag{3.3}$$

$$\dot{w}_{m_i} = \frac{T_{ae_i} - k_{s_i}\gamma_i - D_{m_i} w_{m_i}}{2H_{m_i}}, \tag{3.4}$$

$$\dot{\gamma}_i = 2\pi f (w_{m_i} - \frac{1}{N_{g_i}} w_{G_i}), \tag{3.5}$$

where f represents the nominal grid frequency, T_i is the torque, γ_i the angular displacement between the two ends of the shaft, w_i is the speed, H_i is the inertia constant, and K_{s_i} is the shaft stiffness. The subscript wt_i denotes variables related to the $i-th$ wind turbine rotor. Similarly, m_i and e_i denote the mechanical and electrical variables related to the i^{th} generator, respectively.
The generator receives the mechanical power from the gearbox through the stiff shaft. The relationship between the mechanical torque and the torsional angle is given by:

$$T_{m_i} = k_{s_i}\gamma_i. \tag{3.6}$$

The gearbox connects the low-speed shaft to the high-speed shaft and increases the rotational speeds from 30-60 rotations per minute (rpm) to about 10001800 rpm, the required rotational speed for most generators to produce electricity.

3.4 Transient Model of Doubly Fed Induction Generator

The transient model of a DFIG is described the following equations:

$$\dot{s}_i = \frac{1}{2H_{G_i}}[T_{e_i} - T_{m_i}], \tag{3.7}$$

$$\dot{E}'_{qr_i} = -\frac{1}{T'_{o_i}}[E'_{qr_i} - (X_i - X'_i)i_{ds_i}] - s_i w_s E'_{dr_i} - w_s \frac{X_{m_i}}{X_{m_i} + X_{r_i}} v_{dr_i}, \tag{3.8}$$

$$\dot{E}'_{dr_i} = -\frac{1}{T'_{o_i}}[E'_{dr_i} + (X_i - X'_i)i_{qs_i}] + s_i w_s E'_{qr_i} + w_s \frac{X_{m_i}}{X_{m_i} + X_{r_i}} v_{qr_i}. \tag{3.9}$$

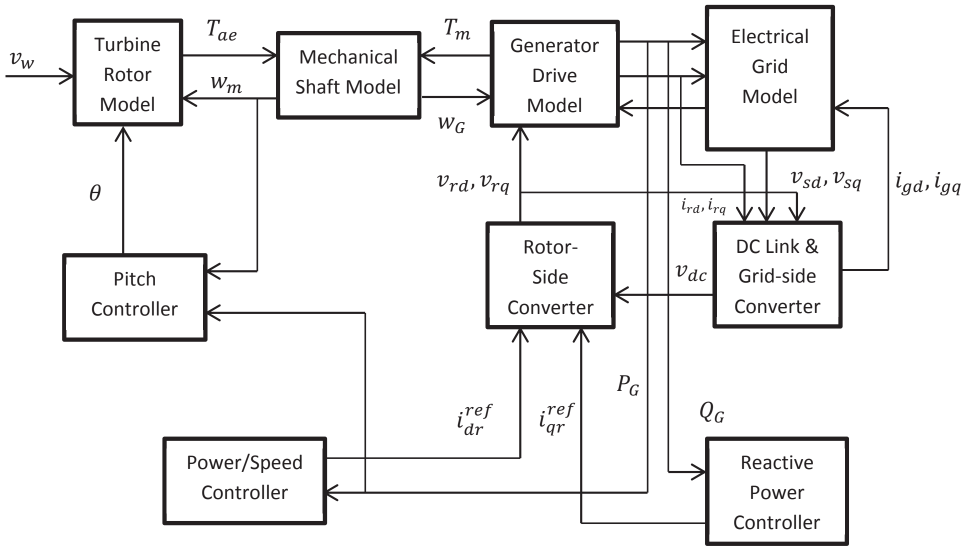

Figure 3.1: Block Diagram of a DFIG Wind Turbine Control System

E'_{dr_i} and E'_{qr_i} is called the rotor back EMF voltages. They reflect the effects of stator dynamics on rotor current dynamics which play an important role in DFIG transient stability. T_{e_i} denotes the electrical torque and T_{m_i} is the mechanical torque with following equations;

$$T_{e_i} = E'_{dr_i} i_{ds_i} + E'_{qr_i} i_{qs_i} \tag{3.10}$$

where $X'_i = \frac{X_{s_i}+X_{m_i}X_{r_i}}{(X_{m_i}+X_{r_i})}$ is the transient reactance, $X_i = X_{s_i} + X_{m_i}$ is the rotor open circuit reactance, $T'_{o_i} = \frac{L_{r_i}+L_{m_i}}{R_{r_i}}$ is the transient open circuit time constant.
The real and reactive power equations are given by;

$$P_{s_i} = V_{ds_i} i_{ds_i} + V_{qs_i} i_{qs_i}, \tag{3.11}$$

and

$$Q_{s_i} = V_{qs_i} i_{ds_i} - V_{ds_i} i_{qs_i}, \tag{3.12}$$

where s_i is the slip, E'_{dr_i} is the $direct-axis$ transient voltage, E'_{qr_i} is the $quadrature-axis$ transient voltage, V_{ds_i} is the $d-axis$ stator voltage, V_{qs_i} is the $q-axis$ stator voltage, T_{m_i} is the mechanical torque, T_{e_i} is the electrical torque, X_{s_i} is the stator reactance, X_{r_i} is the rotor reactance, X_{m_i} is the magnetizing reactance, R_{s_i} is the stator resistance, R_{r_i} is the rotor resistance, H_{m_i} and H_{G_i} are inertia constant constants, D_{m_i} and D_{G_i} are torsion damping, $\delta_i = \int_0^t w_{r_i} dt$, is the rotor angle, w_{r_i} is the rotor speed, w_s is the synchronous speed, i_{ds_i} and i_{qs_i} are $d-axis$ and $q-axis$ components

of the stator current, respectively.
Moreover, the d-q axis component of the rotor current in the transient line can be written as:

$$i_{d_i} = \sum_{j=1}^{n}[E'_{dr_j}(G_{ij}\cos\delta_{ji} - B_{ij}\sin\delta_{ji}) + E'_{qr_j}(G_{ij}\sin\delta_{ji} + B_{ij}\cos\delta_{ji})] \quad (3.13)$$

and

$$i_{q_i} = \sum_{j=1}^{n}[E'_{dr_j}(G_{ij}\sin\delta_{ji} + B_{ij}\cos\delta_{ji}) + E'_{qr_j}(G_{ij}\cos\delta_{ji} - B_{ij}\sin\delta_{ji})] \quad (3.14)$$

3.5 DFIG Behaviour in Different Modes

Reference [40] has studied the effects of rotor currents magnitude during voltage dips on the DFIG dynamic behaviour. This section assumes that rotor speed remains constant during operation. By recalling the induction generator equations, (3.15) and (3.16) are introduced as the stator and rotor voltage at the reference frame.

$$v_s^s = R_s i_s^s + p\lambda_s^s, \quad (3.15)$$

$$v_r^r = R_r i_r^r + p\lambda_r^r. \quad (3.16)$$

In the next step, we write the stator current in terms of the stator flux linkage and the rotor current as (3.18) and (3.17) where is the leakage factor.

$$i_s^s = \frac{1}{L_s}(\lambda_s^s - L_m i_r^s) \quad (3.17)$$

$$\lambda_r^r = \sigma L_r i_r^r + \frac{L_m}{L_e}\lambda_s^r \quad (3.18)$$

By substituting (3.17) in (3.15) and (3.18) in (3.16), the dynamic equations of the stator and the rotor can be written as (3.19) and (3.20), where e_r^r is the system error defined in (3.21).

$$v_s^s = -R_s\frac{L_m}{L_s}i_r^s + (\frac{R_s}{L_s} + p)\lambda_s^s, \quad (3.19)$$

$$v_r^r = (R_r + p\sigma L_r)i_r^r + e_r^r, \quad (3.20)$$

$$e_r^r = \frac{L_m}{L_s}p\lambda_s^r. \quad (3.21)$$

The voltage drop can be defined as $R_r + p\sigma L_r$, where σL_r is function of transient inductance, and R_r is the rotor resistance. The error in (3.21) is

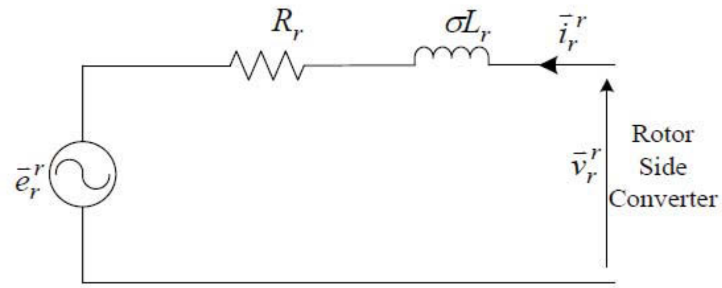

Figure 3.2: DFIG Rotor Equivalent Circuit
[43]

defined because of variation of stator flux,λ_s^r, which suffers from the rotor internal voltage. Note that all the above equations have been expressed based on the open circuit model [40].
As depicted in Figure 3.2, the magnitude of the rotor current depends on:

- Internal rotor voltage;
- Terminal rotor voltage controlled by the RSC;
- Transient inductance and rotor resistance.

From (3.20), it is expected that if the error exceeds, a large rotor current will be produced.

3.5.1 DFIG Behaviour During Normal Operation

The stator voltage and stator flux linkage can be written as (3.22) by neglecting R_s with a constant of speed w_e.

$$\lambda_s^s = \frac{\sqrt{3}\hat{v}_s}{jw_e} e^{jw_e t} \tag{3.22}$$

From (3.22) and (3.21), the flux linkage and the error are expressed in (3.23) and (3.24), where $s = \frac{w_e - w_r}{w_e}$.

$$\lambda_s^r = \frac{\sqrt{3}\hat{v}_s}{jw_e} e^{jw_e t_e - jw_r t}, \tag{3.23}$$

$$e_r^r = (\frac{L_m}{L_s} s\sqrt{3}\hat{v}_s) e^{j(w_e - w_r)t}. \tag{3.24}$$

By assuming $L_m \approx L_s$, the system error in the DFIG form can be approximated by (3.25) which is proportional to the slip during normal operation [40]:

$$|e_r^r| \approx |s|\sqrt{3}v_s. \tag{3.25}$$

3.5.2 DFIG Behaviour Under Voltage Dips

Normally, the fault that occurs at DFIG terminals is known as a bolted three phase fault. In this case, the stator voltage is assumed to be zero for $t > 0$. By neglecting the term $R_s \frac{L_m}{L_s} i_r$, the stator dynamic is given by:

$$(\frac{R_s}{L_s} + p)\lambda_s^s = v_s^s = 0 \Leftrightarrow \begin{cases} \frac{R_s}{L_s}\lambda_{ds}^s + p\lambda_{ds}^s & = 0 \\ \frac{R_s}{L_s}\lambda_{qs}^s + p\lambda_{qs}^s & = 0 \end{cases} \tag{3.26}$$

To solve (3.26), the initial condition in the d-q direction is introduced as:

$$\lambda_s(0) = \lambda_{ds}(0) + j\lambda_{qs}(0) \tag{3.27}$$

It is commonly accepted that the natural stator flux component is a fixed vector during full voltage dip where the amplitude decreases exponentially to zero by considering stator time constant τ_s. Moreover, in this case, the rotor speed is defined as:

$$w_r = (1 - s)w_e \tag{3.28}$$

Hence, after the full voltage dip, the rotor internal error is given by:

$$e_r^r = -\frac{L_m}{L_s}\frac{\sqrt{3}\hat{v}_s}{jw_e}(\frac{1}{\tau_s} + jw_r)e^{-\frac{t}{\tau_s}}e^{-jw_r t}, t \geq 0 \tag{3.29}$$

Naturally, $\frac{1}{\tau_s}$ is smaller than the rotor speed besides assuming $L_m \approx L_s$ so that the maximum magnitude of rotor internal voltage can be approximated as;

$$|e_r^r(t = 0)| \approx (1 - s)\sqrt{3}v_s \tag{3.30}$$

It can be seen that the rotor internal voltage is proportional to $(1 - s)$, where s is the slip of DFIG and $-0.3 < s < 0.2$.

From the above analysis, it is necessary to protect the converter components, such as dc-link and rotor side converter. The reason of this is the overvoltage and overcurrent, which may exceed the maximum voltage produced by the rotor side converter.

Chapter 4

Power System Stability and Voltage Stability

4.1 Introduction

Voltage stability is defined as the ability of the power system to sustain voltages secure at all buses. On the other hand, a power system must have the ability to restore balance between requested load and supplied load even when facing disturbances and grid faults. Voltage instability is caused by the loss of load in transmission lines.
In addition, there is another complex task which is known as a voltage collapse. It is the process that shows classification of events supplementary voltage instability in a major part of a power system. Note that the principle signs of voltage collapse can be emerged because of heavily loaded systems, heavy reactive power flows, inadequate reactive support and load voltage profile. The collapse happens quickly by low-probability single or multiple possibilities. In the case of a sudden increase in reactive power, another probability will occur so that can be met by compensator and generators.
Reactive power plays an important role to keep the power system stable even during grid fault and disturbances. However, the lack of reactive power causes voltage collapse and leads to partial or total shut down of the power system.

4.2 Power System Stability and Wind Power Generations

Voltage stability is mainly because of a large amount of reactive power absorbed by wind turbines during operation under grid faults. However,

voltage stability problem affects safety and operation of power grids and wind farms [71].
Clearly, each type of wind turbine is treated in different way during grid faults and disturbances. Induction motors and induction generators have the same behaviour to absorb reactive power during grid faults that leads to deteriorate voltage stability. Furthermore, variable speed wind turbines equipped with doubly fed induction generators are widely used because of their many advantages in voltage control and reactive power capabilities. Note that the significant advantage of DFIGs is the ability to regulate their own reactive power to control grid voltage or operate at a specified power factor.
However, it is not easy to match the voltage control capability of DFIGs with a synchronous generator due to the capacity limitation of Pulse-Width-Modulation (PWM). The reason of this difficulty refers to the requirement of voltage control which also affects voltage stability if the requirement beyond to the DFIG capability [72].

4.3 Voltage Stability and Nonlinearity

Voltage stability analysis is essential for the following reasons:

- The power generation is centralised in fewer and larger power plants, which means fewer voltage controlled buses, and longer power electrical distances between generation and load;
- The system operates closer to its limits;
- The voltage instability caused by line and generator outages;
- Shunt capacitor compensation is used extensively;
- Induction generators are integrated on a large-scale;
- many incidents having occurred throughout the world such as France, Sweden, USA, Belgium, Japan, etc. [73, 74].

4.3.1 Main Causes of Voltage Instability

The main reason of voltage instability is the loads. Moreover, voltage stability is a truly difficult task that is caused by the nonlinear behaviour of the power system. The system nonlinearity increases when the stress on the system increases. It is necessary to take the nonlinear behaviour of power system devices into account during the design and analysis of the controllers.

Loads are the main cause of voltage instability in response the consumed power and diturbances. The loads increase the stress on high voltage network, leading to an increase in the reactive power consumption by power system devices. This augmentation causes additional voltage reduction [112, 113].
Another main problem in voltage stability is the voltage drop. It happens when both active and reactive power trill, through the inductive reactance of transmission network. This limitation is in terms of voltage support and power transfer which make it understandable to see the effectiveness of the reactive power factor.

4.4 Control Levels of DFIGs based on Wind Turbine

Figure 4.1 illustrates the control levels of wind turbine equipped with DFIG. The aim of each control level is described as follows:

- The first level regulates the power flow between grid and generator.
- The second level controls the amount of energy extracted by the wind turbine rotor.
- The third level responds to the wind farm or grid-connected central control commands for MW dispatch, voltage frequency or inertial control.

A maximum reactive power can be achieved by updating the reactive power with real power and actual terminal voltage. It is the main objective of this study.

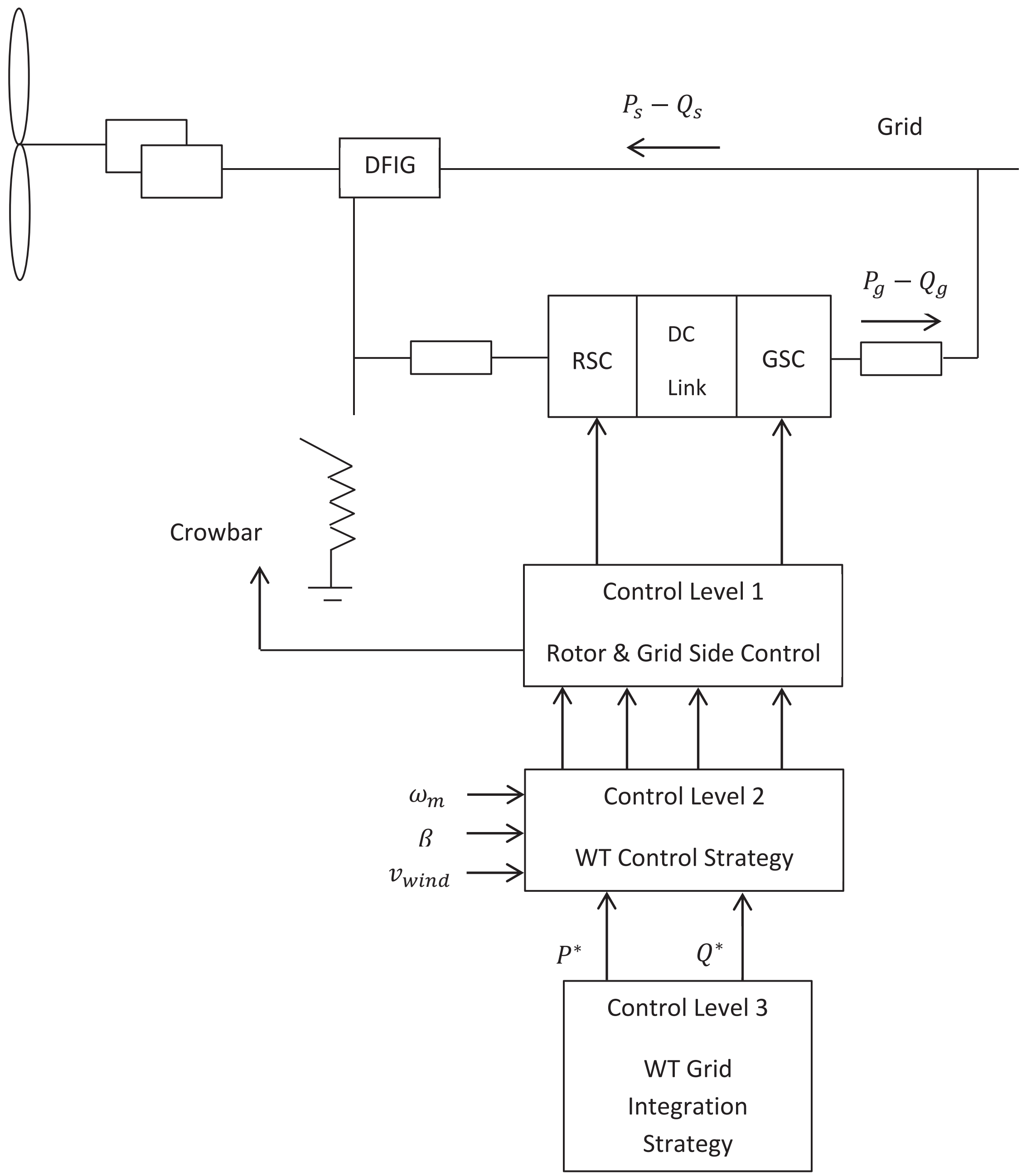

Figure 4.1: Control Levels of DFIGs based on WT

Chapter 5

Model Predictive Control of DFIG-based Wind Turbine

5.1 Introduction

Model Predictive Control (MPC) is a powerful control method due to its ability to handle multivariable systems and to incorporate constraints through problem formulation [76, 78, 79]. MPC algorithms have been used in the chemical process industry and also applied in different industrial control problems [75]. Recently, they are reported to be used in power and renewable energy systems as well [46, 77].

Unlike other classical methods, MPC includes an online optimization algorithm. The optimization part employs an internal control loop to predict system behaviour so that the control objective can be formulated in a cost function. The bounds and system limitations are expressed in the constraints. At each sampling time, an optimization problem is solved to find an optimal input sequence. Based on the MPC concept, just the first element is operated to the plant. As shown in Figure 5.1, for the next step, the time is shifted by one step and the optimization procedure can be repeated over the shifted time. The updated control input introduces feedback to MPC at each control step referred a receding horizon policy by solving a new optimization problem.

The MPC procedure is shown in Figure 5.2 and it can be summarized as follows:

- Measure (estimate) the states at the current time step.

- Obtain the optimal control sequence by solving the optimization problem over the prediction horizon.

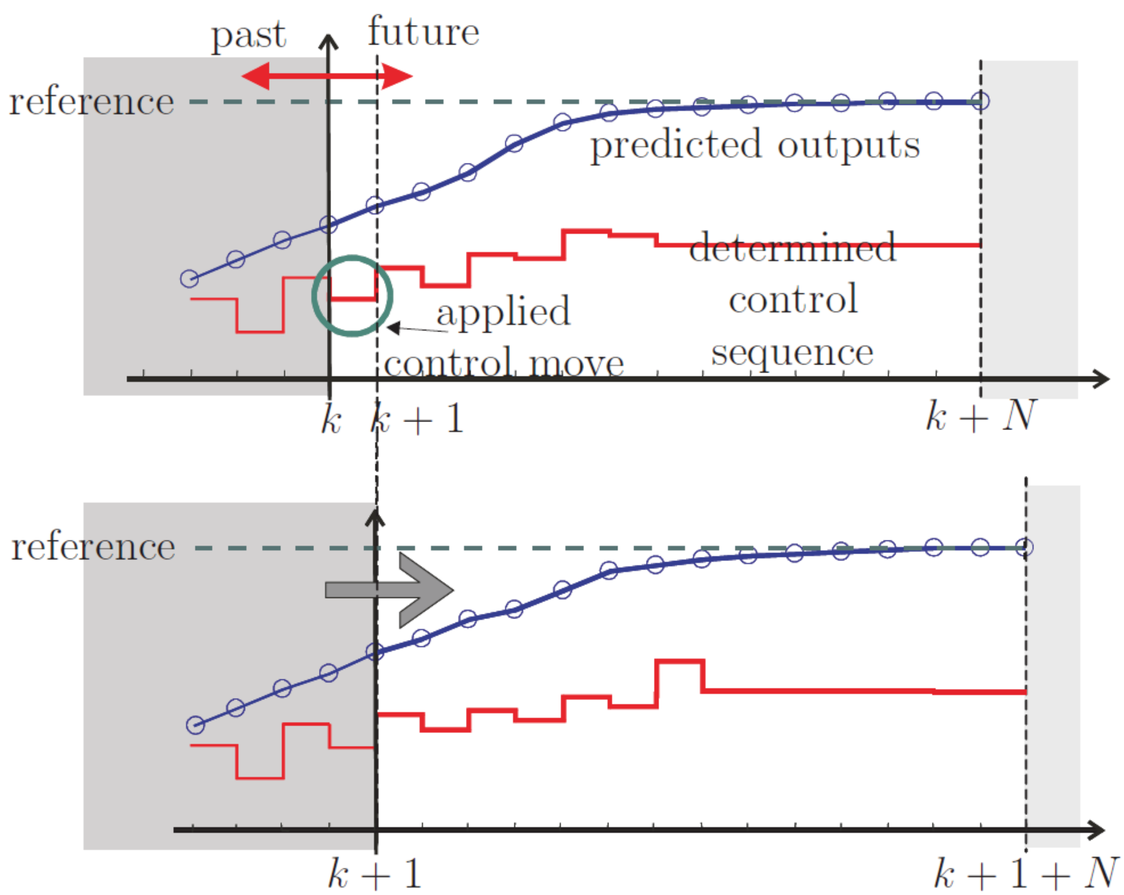

Figure 5.1: The Receding Horizon Policy

- Apply the first element of the optimal control sequence.

- Repeat the whole procedure in the next time step.

Wind energy has the fastest growing rate among renewing energies, with annual growth rate over 20% [80]. The size and nominal power capacity of wind turbines are continuously increased to achieve a more competitive energy cost compared to conventional sources. To maintain this growth, the performance of wind turbines has to be improved. Modern wind turbines are equipped with doubly-fed induction generator (DFIGs). The most important benefit of this equipement, is that it can handle 20-30% of the total system power which leads to reducing the losses in the power electronic equipment [81, 82]. Moreover, because of DFIG capability in decoupling the control of power (active and reactive), these types of generators have a better behaviour in system stability during short circuit faults compared with induction generators [83].
In the engineering fields, PID controllers are well accepted because of their simplicity and reliablity. They are the typical techniques to regulate the wind power. In contrast, because of inherent nonlinear characteristics which there are in dynamic of the wind and turbine, large response time and also difficulties to find appropriate PID parameters in a systematic way, these types of controllers tend to care less and less [84]. However, the performance of dynamic control cannot be guaranteed during transients between WT and DFIG [87]. To reach a better control performance in transient stability of power systems, it is necessary to investigate the new controller design methods for the WT with DFIG system, especially when the system is under large disturbances.
The main objetive of the control system in this area is to reduce electrical power and rotor speed fluctuations while reducing the control loads. References [88]- [89] have developed control strategies of DFIGs wind turbines based on optimum power efficiency for low wind speeds. In high wind speed, the power system requires that DFIGs wind turbines operate with generation limits for both active and reactive power which depends on the generation capability and the grid power needs [90]. [91] has proposed an algorithm to control active power by acting on the blade pitch angle limits. Recently, [92] has noted that this technique leads to large mechanical stress on the WT system; and consequently, the energy captured by the turbines is not optimal due to the effect of the pitch systems.
The main goal of control system wind turbine with DFIG is to control the output power to track the optimum power operation of wind turbines the aim is to limit the output power value at the rated power for high speed winds and to control the delivered reactive power to the grid [89]. With new generation of actuators, wind turbines are becoming bigger and more

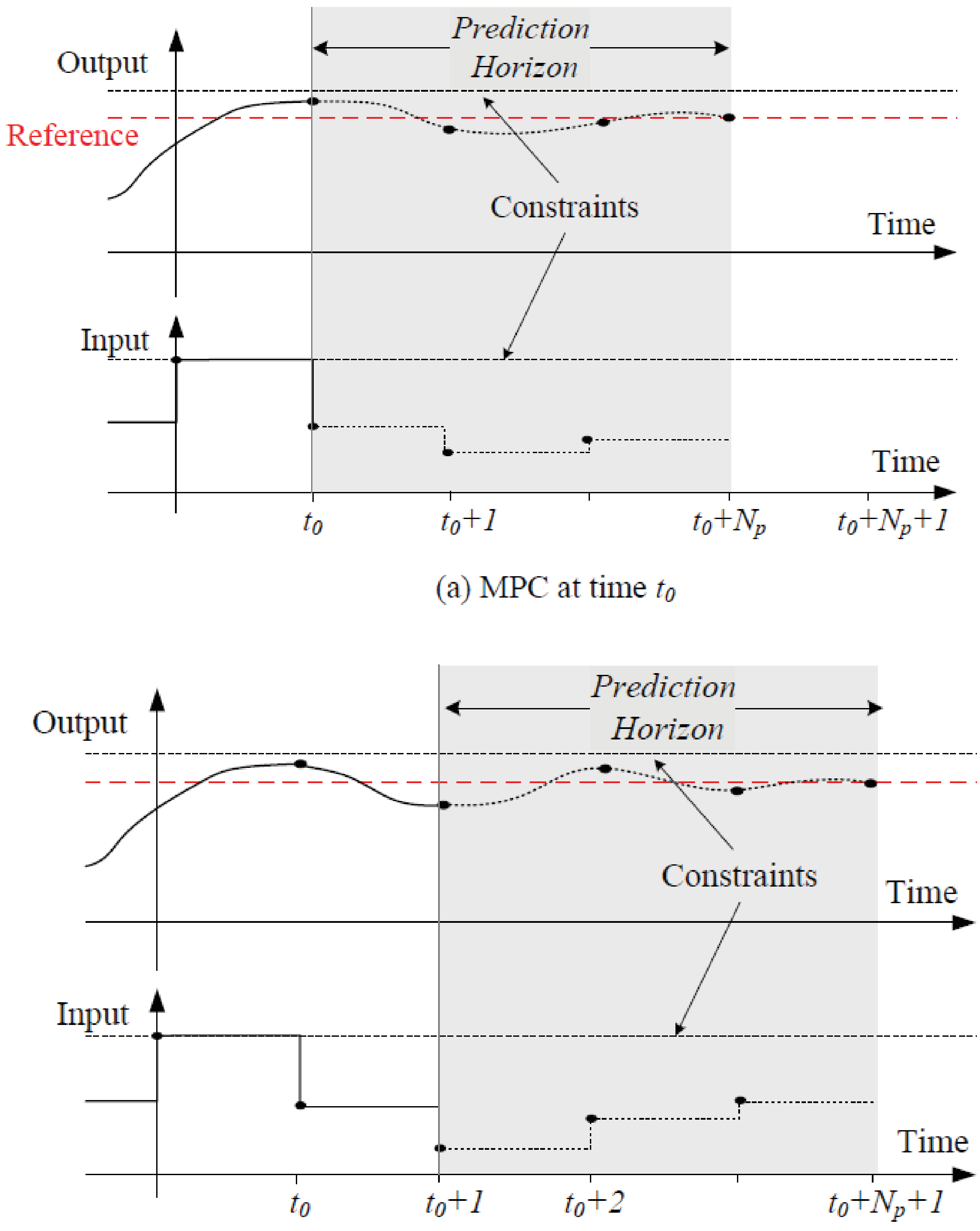

(a) MPC at time t_0

(b) MPC at time t_0+1

Figure 5.2: Concepts of Model Predictive Control

flexible. The turbine is treated as a MIMO [92]. However, the challenge will appeared when we see the difficulties to specify different objectives and design controllers based on paired input/output channels. Model Predictive Control (MPC) algorithms have been used in the chemical process industry and then their application gained in different types of industrial control problem [93]. Recently, they are reported to be used in power and renewable energy systems as well [94], [95]. A control scheme for load management is proposed in [96]. The work of [97] has presented MPC for wind turbine load reduction based on different linearized state-space models. MPC algorithms are effective when the wind turbine is modelled as a Multi-Input-Multi-Output (MIMO) systems (see [98]).
A MIMO control system is studied in [99]. Reference [100] has proposed a strategy which is based on MPC. Recently, [101] has designed a corrective control based on MPC to correct out-of-limits voltages by applying optimal changes of the control variables wich are active power, reactive power and terminal voltage.
Dynamic of transition from the measured to the target values must be considered through the design of robust corrective controllers [101]. However, since single step optimization cannot satisfy system stability, multi step optimization is proposed (see e.g., [102], [103]).
The main advantages of the MPC include handling of MIMO control problems, taking into account the actuator limitation and constraints of system variables, inherent optimization of a specified system criterion which make it so practical [104].

5.1.1 Turbine Modelling with DFIG

The WT system consists of a drive train and DFIG. The drive train of the WT system is represented by one-mass model [85], while the DFIG is represented by a third-order model as follows:
Dynamic Equations:

$$2H_{tot}\frac{ds}{dt} = P_s - P_m, \tag{5.1}$$

$$\frac{dE'_q}{dt} = -sw_sE'_d + w_s\frac{L_m}{L_{rr}}v_{dr} - \frac{1}{T'_0}[E'_q - (X_s - X'_s)i_{ds}], \tag{5.2}$$

$$\frac{dE'_d}{dt} = sw_sE'_q - w_s\frac{L_m}{L_{rr}}v_{qr} - \frac{1}{T'_0}[E'_d + (X_s - X'_s)i_{qs}], \tag{5.3}$$

where

$$
\begin{aligned}
X_s =& w_s L_{ss} = x_s + X_m, \\
X_s' =& w_s (L_{ss} - L_m^2 / L_{rr}), \\
T_0' =& L_{rr} / R_r.
\end{aligned}
$$

Electrical Equations:

$$P_s = - E_d' i_{ds} - E_q' i_{qs}, \tag{5.4}$$

$$Q_s = E_d' i_{qs} - E_q' i_{ds}, \tag{5.5}$$

$$E_d' = - r_s i_{ds} + X_s' i_{qs} + v_{ds}, \tag{5.6}$$

$$E_q' = - r_s i_{qs} - X_s' i_{ds} + v_{qs}, \tag{5.7}$$

where s is the rotor slip; H_{tot} is the total inertia constant of the turbine and generator; P_s is the output active power of the DFIG stator; P_m is the WT mechanical power; L_{ss} is the stator self-inductance; L_{rr} is the rotor self-inductance; L_m is the mutual inductance; w_s is the synchronous angle speed; X_s is the stator reactance; X_s' is the stator transient reactance; E_d' and E_q' are the d and q axis voltages behind the transient reactance, respectively; T_0' is the rotor circuit time constant; i_{ds} and i_{qs} are the d and q axis stator currents, respectively; v_{ds} and v_{qs} are the d and q axis stator terminal voltages, respectively; v_{dr} and v_{qr} are the d and q axis rotor voltages, respectively; and Q_s is the reactive power of the stator of the DFIG. Equations (5.1)-(5.3) shows the third-order DFIG model. Figure 5.3 shows the schematic diagram of DFIG.
Indeed, the state of the system is

$$\Delta x = [\Delta S, \Delta E_q', \Delta E_d']^T, \tag{5.8}$$

and the output variables are:

$$
\begin{aligned}
y_1 =& s - s_0, \\
y_2 =& v_t - v_{t,ref} = \sqrt{v_{ds}^2 + v_{qs}^2} - v_{t,ref},
\end{aligned} \tag{5.9}
$$

where v_t is the terminal voltage of the wind turbine with DFIG and $v_{t,ref}$ is the control reference of the terminal voltage of the WT and DFIG normally chosen as 1 p.u. v_{qs} becomes zero in aligning the d axis of the $d-q$ reference with the direction of the terminal voltage. By substituting (5.6) into (5.9) we have

$$y_2 = v_{ds} - v_{t,ref} = E_d' + r_s i_{ds} - X_s' i_{qs} - v_{t,ref}. \tag{5.10}$$

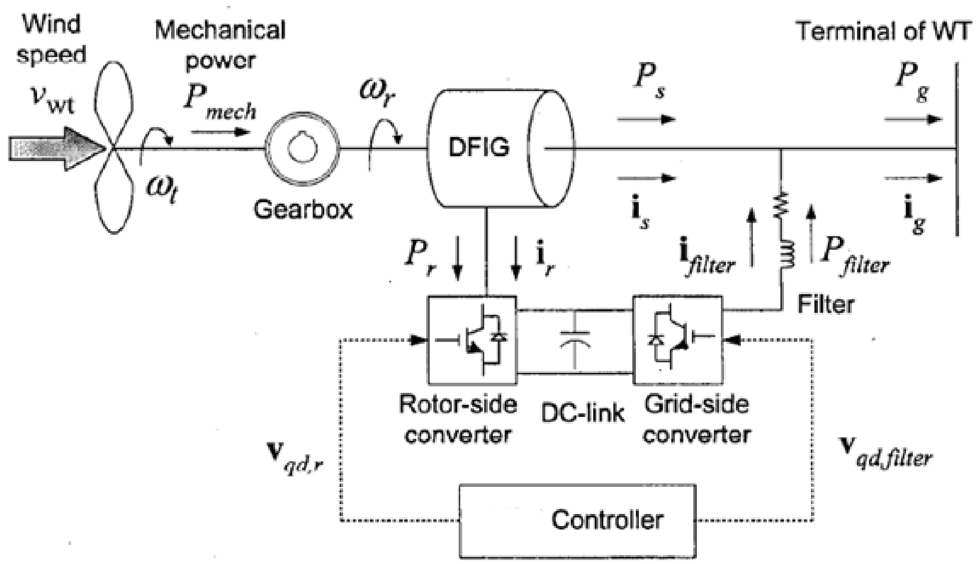

Figure 5.3: Schematic Diagram of a DFIG

5.1.2 Model Exact Linearization of the WT with DFIG

Based on [87], the model of the wind turbine with DFIG is linearized as follows:

$$\dot{z_1} = z_2, \tag{5.11}$$

$$\dot{z_2} = v_1 = \frac{1}{2H_{tot}}(-\dot{E}'_d i_{ds} - \dot{E}'_q i_{qs}), \tag{5.12}$$

$$\dot{z_3} = v_2 = \dot{v_{ds}}. \tag{5.13}$$

By substituting the dynamic equations (5.2)-(5.3) into the above equations, we have:

$$\dot{z_1} = z_2, \tag{5.14}$$

$$\begin{aligned}\dot{z_2} = v_1 = &-\frac{1}{2H_{tot}w_0}[sw_s E'_q i_{ds} - sw_s E'_d i_{qs} - \frac{1}{T'_0}(E'_d i_{ds} + E'_q i_{qs})] \\ &- \frac{L_m}{2H_{tot}L_{rr}} w_s (v_{dr} i_{qs} - v_{qr} i_{ds}),\end{aligned} \tag{5.15}$$

$$\dot{z_3} = v_2 = sw_s E'_q - \frac{1}{T'_0}[E'_d + (X_s - X'_s) i_{qs}] - \frac{L_m}{L_{rr}} w_s v_{qr}. \tag{5.16}$$

5.2 Control Design Algorithm

It is stated in [105] that the maximum reactive power can be achieved by updating the reactive power with active power and actual terminal voltage.

Also the reactive power can be set for each generator. Hence, the control scheme in this work calculates only the change of power output of the distributed energy sources (P_g, Q_g), where P is the active power and Q is the reactive power, and the point of common coupling V_{PCC} at the power supply point to maintain the monitored voltages within desired limits. The change of control variables at time k is:

$$\Delta u(k) = [\Delta P_g(k), \Delta Q_g(k), \Delta V_{PCC}(k)]^T, \tag{5.17}$$

where $\Delta u(k) = u(k) - u(k-1)$, and ^{T} denotes array transposition. Figure 5.4 presents the basic concept of MPC, where the controller is updated at time $k+1$ with a new set of measurements to control actions that have been applied at and before time k [106]. The overall objective is to minimize the change of control variables while satisfying the voltage limits. This leads to the following standard Quadratic Programming (QP) problem:

$$\begin{aligned} min \sum_{i=0}^{N_p-1} [(x_i - x_{ref,i})^T Q_x (x_i - x_{ref,i}) + (u_i - u_{ref,i})^T \\ Q_u (u_i - u_{ref,i})] + (x_{N_p} - x_{ref,N_p})^T S (x_{N_p} - x_{ref,N_p}) \end{aligned} \tag{5.18}$$

subject to the equality and inequality constraints:

$$\begin{aligned} u_{min} \leq & u(k+i) \leq u_{max}, \quad \text{for } i = 0, \cdots, N_p - 1 \\ y_{min} \leq & H x_i \leq y_{max}, \qquad \text{for } i = 1, \cdots, N_p. \end{aligned} \tag{5.19}$$

Under some conditions, it is infeasible to bring voltages within the normal operation constraints. This circumstance may happen under the following estates [101]:

- Reaching maximum or minimum power output in DG units
- Being very far from the desired operation point, voltage values, which happens after a disturbance
- Because of strict voltage constraints, it is impossible to operate with all voltages within bounded constraints.

In order to overcome this shortage, the following condition is proposed:

$$\Delta u_{min} \leq \Delta u(k+i) \leq \Delta u_{max} \tag{5.20}$$

for $i = 0, 1, \cdots, N_c - 1$. From a practical view, we have:

$$\begin{aligned} V_{min} \leq & V(k+i|k) \leq V_{max} \\ V_{min} = & V(k+i-1|k) + \frac{\partial V}{\partial u} \Delta u(k+i-1), \end{aligned} \tag{5.21}$$

for $i = 1, \cdots, N_p$. Here, $N_p \geq N_c$, R is a weight matrix used to penalize the control variable u, and $\Delta u(k+i) = 0$ for $i \geq N_c$. Finally, $V(k+i|k)$ is the set of predicted bus voltage given the measurements at time instant k, and $\frac{\partial V}{\partial u}$ is the sensitivity matrix of bus voltages with respect to the control variables.
The controller is updated by the real-time measurements of bus voltage magnitude $V(k|k)$, and the previous control signals $u(k-1)$.
Based on the QP problem, only free variables u are allowed as below:

$$\min_u u^T H u + h^T u; \text{ s.t } Lu \leq b \tag{5.22}$$

where H is the Hessian and L are constant matrices, h and b are constant vectors, and u is a vector variable. Therefore, translating the objectives and constraints for x into the corresponding objectives and constraints of u is essential. Consequently, the states x_i, $i = 1, \cdots, N_p$ as a function of the current state x_0 for $i = 0, \cdots, N_p - 1$ are advised by applying the state-space model (5.23) repeatedly for $i = 0, \cdots, N_p$:

$$x = \underbrace{\begin{pmatrix} A \\ A^2 \\ \vdots \\ A^{N_p-1} \\ A^{N_p} \end{pmatrix}}_{\hat{A}} x_0 + \underbrace{\begin{pmatrix} B & 0 & \cdots & 0 & 0 \\ AB & B & \cdots & \vdots & \vdots \\ \vdots & \vdots & \ddots & 0 & 0 \\ A^{N_p-2}B & A^{N_p-3}B & \cdots & B & 0 \\ A^{N_p-1}B & A^{N_p-2}B & \cdots & AB & B \end{pmatrix}}_{\hat{B}} u \tag{5.23}$$

The controller must bring the controlled voltage inside the limits defined by the normal operation constraints. Very recently, [101] has formulated a linear variation due to calculate the limitations as follows:

$$V_{min}(k+i) \leq V(k+i|k) \leq V_{max}(k+i), \tag{5.24}$$

where

$$V_{min}(k+i) = (1 - \frac{N_p - i}{\rho N_p})V_{min}, \tag{5.25}$$

$$V_{max}(k+i) = (1 + \frac{N_p - i}{\rho N_p})V_{max}, \tag{5.26}$$

for $i = 1, \cdots, N_p$ and ρ is a tuning parameter used to modulate the rate of change of the voltage limits in the horizon. In the next section, we will explain the control process under study in more details.

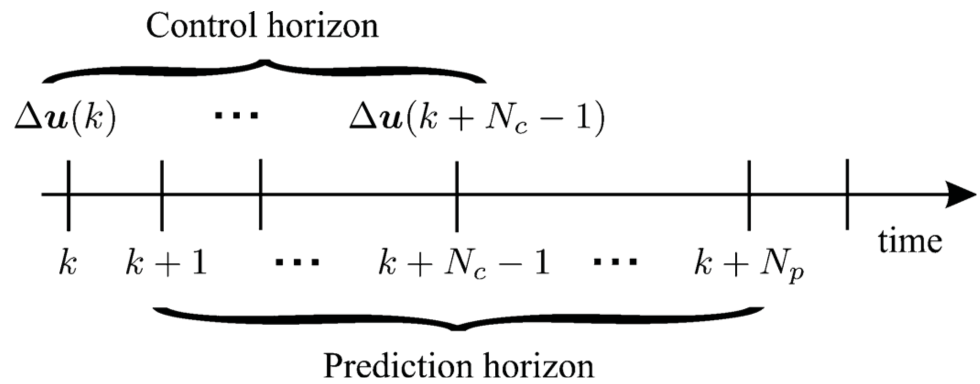

Figure 5.4: Basic Concept of Multi-step Optimization with Horizons

5.3 Controller Performance Evaluation

5.3.1 Task Description

The electrical equations (5.4)-(5.7) describe the relationship between the active powers of rotor and stator of the DFIG. The regulation of the required reactive power between DFIG and the grid can be tuned by the dc link, as depicted in Figure 5.3. On the other hand, v_{dr} and v_{qr} play important roles in increasing the efficiency and safety of the system. The problem occurrs in the case of faulty systems and when the voltage values become far from the normal operating values which exceed the capacity of the feedback converter. Therefore, rotor voltage, v_{dr} and v_{qr} must be limited to overcome this shortage. MPC is successfully employed as demonstrated by the simulation results in Figure 5.5. It is showed that a wind turbine with DFIG under this control strategy can actively participate in the power network because of the reliablity in active and reactive power control according to constrained power limitations.

5.3.2 Simulation Result

To translate the input constraints, we have;
$\chi = \chi_{dev} + \chi_v$, where $\chi_{dev} = \hat{A}x_0 + \hat{B}u_{ref} - x_{ref}$. Note that matrices $\hat{A}$ and $\hat{B}$ are calculated in (5.23).
The first term of (5.18) is not affected by the optimization and can be left out of the objective function

$$\tilde{f}(\chi, v) = 2\chi_{dev}^T \hat{Q}_x \chi_v + v^T \hat{Q}_u v, \tag{5.27}$$

where $\chi_v = \hat{B}v$. We express the corresponding QP-matrices as:

$$\begin{aligned} H &= \hat{B}^T\hat{Q}_x\hat{B} + \hat{Q}_u \\ h^T &= \chi_{dev}^T\hat{Q}_x\hat{B} \end{aligned} \tag{5.28}$$

and rewrite the objective function (5.22) as:

$$v^T Hv + h^T v, \tag{5.29}$$

where the contribution form $v = u - u_{ref}$ is defined as $\chi_v = \hat{B}v$.
We introduce

$$\hat{Q}_x = \begin{pmatrix} Q_x & 0 & \cdots & 0 & 0 \\ 0 & Q_x & \ddots & \vdots & \vdots \\ 0 & 0 & \ddots & 0 & 0 \\ \vdots & \vdots & \ddots & Q_x & 0 \\ 0 & 0 & \cdots & 0 & S, \end{pmatrix},$$

$$\hat{Q}_u = \begin{pmatrix} Q_u & 0 & \cdots & 0 & 0 \\ 0 & Q_u & \ddots & \vdots & \vdots \\ 0 & 0 & \ddots & 0 & 0 \\ \vdots & \vdots & \ddots & Q_u & 0 \\ 0 & 0 & \cdots & 0 & Q_u \end{pmatrix},$$

$Q_x = C^T Q_y C$ and set $N_p = N - 1 -$ prediction horizon.
To translate the state constraints, the upper and lower constraints must be defined. Hence, (5.30) and (5.31) are given for the upper and lower constraints, respectively.

$$\begin{pmatrix} H & 0 & \cdots & 0 & 0 \\ 0 & H & \ddots & \vdots & \vdots \\ 0 & 0 & \ddots & 0 & 0 \\ \vdots & \vdots & \ddots & H & 0 \\ 0 & 0 & \cdots & 0 & H \end{pmatrix} \chi_v \leq \begin{pmatrix} y_{max} \\ y_{max} \\ \cdots \\ y_{max} \end{pmatrix} - \begin{pmatrix} H & 0 & \cdots & 0 & 0 \\ 0 & H & \ddots & \vdots & \vdots \\ 0 & 0 & \ddots & 0 & 0 \\ \vdots & \vdots & \ddots & H & 0 \\ 0 & 0 & \cdots & 0 & H \end{pmatrix} (\chi_{dev} + x_{ref}) \tag{5.30}$$

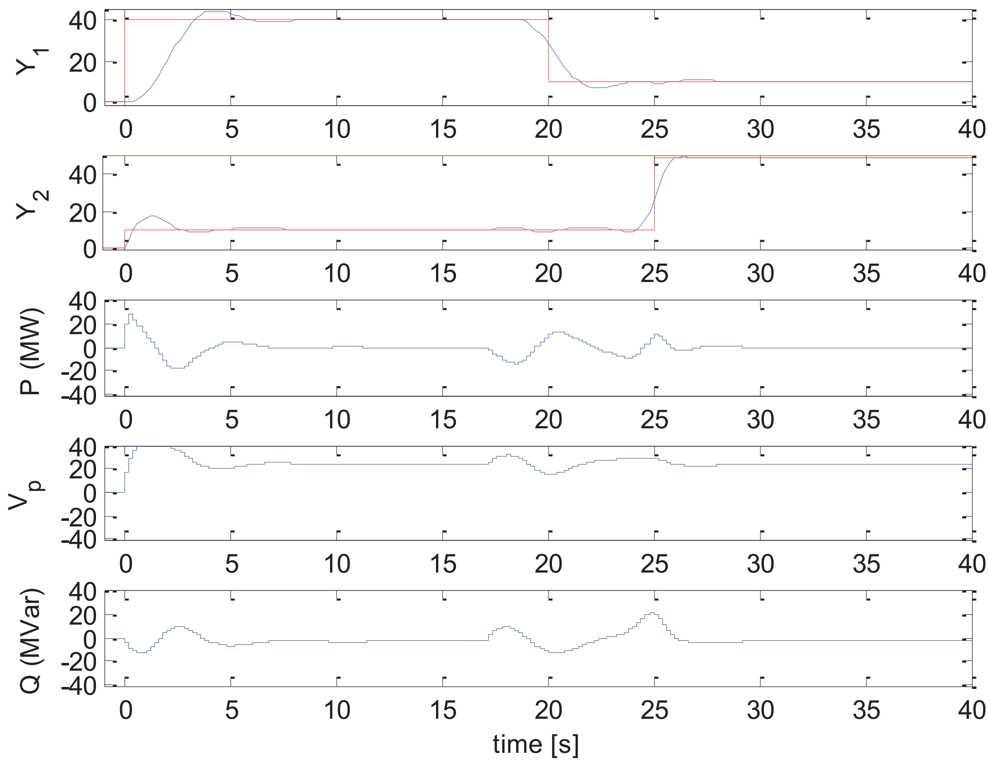

Figure 5.5: Plot of Results

If $\hat{H} = diag(H)$, we have:

$$-\hat{H}\chi_v \leq -\begin{pmatrix} y_{min} \\ y_{min} \\ \cdots \\ y_{min} \end{pmatrix} + \hat{H}(\chi_{dev} + x_{ref}). \tag{5.31}$$

Figure 5.5 shows the response of the system variables to step changes in the reference bus voltage from 1.00 (p.u) to 0.95 (p.u) and back to 1.00 (p.u). As seen, v_t follows its reference value very closely. In our work, the sampling time is chosen as 0.2 and the horizon is $N_p = 15$. The wind turbine parameters are given in [85].

5.4 Conclusion

In this chapter, a multivariable control scheme based on model predictive control (MPC) is presented. Multi-step optimization is employed in order to update and correct the control action in real time measurements. The problematic voltages are brought as close as feasible to the normal operating points, resulting minimalchanges of the control variables.

Chapter 6

Conclusion and Future Work

6.1 Conclusion

In this study, the importance of wind energy is surveyed. Growing wind energy demand in New South Wales is also discussed based on government reports. Then, a brief overview of wind energy conversion systems is given, including descriptions of the main components of wind turbines, power captured from the wind and turbine and also the classification of wind turbines. The significance of Doubly Fed Induction Generators (DFIGs)is studied in parallel with describing the challenges controlling the levels of wind turbine and generator. Moreover, the dynamic behaviour of DFIGs is studied under different modes including normal operation and under voltage dips.

All of the principle components are modelled and discussed, including the aerodynamic system of wind turbine, rotor model and shaft model. Then, the dynamic model of DFIG-based wind turbine is given by a third-order model of one-mass wind turbine.

The main purpose in power network is to deliver smooth voltage even in case of fault occurrance. Therefore, grid requirements topic is detailed, such as the capability of power and frequency quality control and reactive power capability.

The stable operation of power system requires the availability of sufficient reactive power generation. In this study, it is concluded that updating reactive power with real power at actual terminal voltage is a suitable solution to reach the maximum reactive power. For this target, new optimization problem applies feedback to Model Predictive Control (MPC) at each control step. In order to guarantee the system stability even in the case of inaccuracies, multi-step optimization is introduced to bring the unhealthy voltages as close as possible to normal operation points minimizing the changes of control variables.

6.2 Future Work

This research has investigated many gates for further works on DFIG-based wind turbines, enhancement of reactive power capability, voltage regulation and improvement of transient stability of power systems.
The potential future work include:

- To study the dynamic model of wind farms at Point Common Coupling (PCC) and evaluate the effectiveness of designed model.

- To consider the inherent nonlinearity of power systems and interactions among wind farms for the class of interconnected systems.

- To design and implement a new control scheme for reactive power compensation, voltage regulation and transient stability enhancement of large-scale grid-connected power systems.

- To achieve a maximum reactive power even in the case of reaching saturation at minimum or maximum voltage limits. This can be done by employing the new bounded control approach designed based on APRC-Based Decentralised Model Predictive Control (DMPC). It may guarantee stability of the network by only local APRC-based controller [114].

Bibliography

[1] W. Qiao, R. G. Harley, and G. Kumar, "Reactive power control of a large wind farm and a STATCOM using heuristic dynamic programming", *IEEE Transactions on Energy Conversion*, vol. 24, no. 2, pp. 493-503, 2009.

[2] M. J. Hossain, H. R. Pota, and C. Kumble, "Decentralized robust static synchronous compensator control for wind farms to augment Dynamic transfer capability", *Journal of Renewable Energy*, vol. 2, pp.1-20, 2010.

[3] L. Xu and C. Wei, "Torque and reactive power control of a doubly fed induction machine by position sensorless scheme", *IEEE Transactions on Industry Applications*, vol. 31, no. 3, pp. 636 -642,1995.

[4] M. J. Hossain, T. K. Saha, N. Mithulananthan, and H. R. Pota, "Control strategies for augmenting LVRT capability of DFIGs in interconnected power systems", *IEEE Transaction on Industrial Electronics*, vol. 60, no. 6, pp. 2510-2522 , 2013.

[5] J. Lopez, E. Gubia, J. Ruiz, and L. Marroyo, "Ride through of wind turbines with doubly fed induction generator under symmetrical voltage dips", *IEEE Transactions on Industrial Electronics*, vol. 56, pp. 4246-4254, 2009.

[6] E. Hau, "Wind turbines; fundamentals, technologies, applications, economics", *Berlin, New York, Springer*, 2006.

[7] T. Shanker, R. K. Singh, "Wind energy conversion system: A review, *IEEE Conference on Engineering and Systems*, pp. 1-6,

2012.

[8] M. Calais,it ENG421 Unit notes. Perth, WA, Australia: Murdoch University

[9] T. Ackermann, "Wind power in power system", *John Wiley & Sons*, 2005.

[10] G. Xiang, W.Gang; W. Zhengrong, and L. Haifeng, "Fault current contributions of doubly fed induction generator wind turbines under different control strategies",*International Conference on Advanced Power System Automation and Protection (APAP)*, vol.2, pp.1209-1214, 2011.

[11] M. Kayikci, J. V. Milanovic, "Reactive power control strategies for DFIG-based plants",*IEEE Transactions on Energy Conversion*, vol.22, no.2, pp.389-396, 2007.

[12] S. Muller, M. Deicke, and R. W. De Doncker, "Doubly fed induction generator systems for wind turbines", *IEEE Industry Applications Magazine*, vol. 8, pp. 26-33, 2002.

[13] H. Li, and Z. Chen, "Overview of different wind generator systems and their comparisons", *IET Renewable Power Generation*, vol. 2, pp. 123-138, 2008.

[14] H. Polinder, F. F. A. Vander Pijl, G. J. De Vilder, "Comparison of direct-drive and geared generator concepts for wind turbines", *IEEE Transactions on Energy Conversion*, vol. 21, pp. 725-733, 2006.

[15] L. H. Hansen, P. H. Madsen, F. Blaabjerg, H. C. Christensen, "Generators and power electronics technology for wind turbines", *In Proc. IEEE Industrial Electronics Society*, pp. 2000-2005, USA, 2001.

[16] R. Datta, and V. T. Ranganathan, "Variable speed wind power generation using dubly fed wound rotor induction machine-a comparison with alternative schemes", *IEEE Transactions on Energy*

Conversion, vol. 17, pp. 414-421, 2002.

[17] I. Munteanu, N. A. Cutululis, A. I. Bratcu, and E. Ceanga, "Optimization of variable speed wind power systems based on a LQG approach", *Control Engineering Practice*, vol. 13, pp. 903-912, 2005.

[18] F. D. Bianchi, H. De Battista, and R. J. Mantz, "Wind turbine control systems; Principles, modelling and gain scheduling design", *London, Springer*, 2007.

[19] W. E. Leithead, and B. Connor, "Control of variable speed wind turbines: Design Task", *International Journal of Control*, vol. 73, pp. 1189-1212, 2000.

[20] E. A. Bossanyi, "The design of closed loop controllers for wind turbines", *Wind Energy*, vol. 3, pp. 149-163, 2000.

[21] P. Novak, T. Ekelund, I. Jovik, and B. Schmidtbauer, "Modelling and control of variable speed wind turbine drive system dynamics", *IEEE Control Systems Magazine*, vol. 15, pp. 28-38, 1995.

[22] L. Y. Pao, K. E. Johnson, "Control of wind turbines", *IEEE Control Systems Magazine*, Vol. 31, pp. 44-62, 2011.

[23] A. D. Hansen, P. Sorensen, F. Lov, and F. Blaabjerg, "Control of variable speed wind turbines with dubly fed induction generators", *Wind Engineering*, vol. 28, pp. 411-443, 2004.

[24] J. Zaragoza, J. Pou, A. Arias, C. Spiteri, E. Robles, and S. Ceballos, "Study and experimental verification of control tunning strategies in a variable speed wind energy conversion system", *Renewable Energy*, Vol. 36, pp. 1421-1430, 2011.

[25] F. D. Bianchi, R. J. Mantz, and C. F. Christiansen, "Control of variable speed wind turbines by LPV gain scheduling", *Wind Energy*, vol. 7, pp. 1-8, 2004.

[26] B. Boukhezzar, and H. Siguerdidjane, “Nonlinear control of a variable speed wind turbine using a two-mass model”, *IEEE Transactions on Energy Conversion*, vol. 26, pp. 149-162, 2011.

[27] B. Boukhezzar, and H. Siguerdidjane, “Comparison between linear and nonlinear control strategies for variable speed wind turbines”, *Control Engineering Practice*, vol. 18, pp. 1357-1368, 2010.

[28] K. E. Johnson, L. Y. Pao, M. J. Balas, and L. J. Fingersh, “Control of variable speed wind turbines: standard and adaptive techniques for maximizing energy capture”, *IEEE Control Systems Magazine*, vol. 26, pp. 261-269, 2012.

[29] B. Beltran, M. E. H. Benbouzid, and T. Ahmed Ali, “Second order sliding mode control of a doubly fed induction generator driven wind turbine”, *IEEE Transactions On Energy Conversion*, vol. 27, pp. 261-269, 2012.

[30] F. D. Bianchi, R. J. Mantz, and C. F. Christiansen, “Power regulation in pitch controlled variable speed WECS above rated wind speed”, *Renewable Energy*, vol. 29, pp. 1911-1922, 2004.

[31] E. B. Muhando, T. Senjyu, A. Yona, H. Kinjo, and T. Funabashi, “Disturbance rejection by dual pitch control and self-tunning regulator for wind turbine generator parametric uncertainty compensation”, *IET Control Theory and Applications*, vol. 1, pp. 1431-1440, 2007.

[32] A. D. Wright, and M. J. Balas, “Design of state-space based control algorithms for wind turbine speed regulation”, *Journal of Solar Energy Engineering, Transactions Of the ASME*, Vol. 125, pp. 386-395, 2003.

[33] K. Z. Ostegaard, J. Stoustrup, and P. Brath, “Linear parameter varying control of wind turbines covering both partial and full load conditions”, *International Journal of Robust and Nonlinear Control*, vol. 19, pp. 92-116, 2009.

[34] O. Anaya-Lara, N. Jenkins, J. Ekanayake, P. Cartwright, M. Hughes, “Wind energy generation: Modelling and Control”, *Chichester, U.K: John Wiley and Sons*, 2009.

[35] F. K. A. Lima, and A. Luna, P. Rodriguez, E. H. Watanable, and F. Blaabjerg, “Rotor Voltage Dynamics in the Dubly Fed Induction generator During Grid Faults”, *IEEE Transactions On Power Electronics*, Vol. 25, pp. 118-130, 2010.

[36] J. Lopez, E. Gubia, E. Olea, J. Ruiz, and L. Marroyo, “Ride through of wind turbines with doubly fed induction generator under symmetrical voltage dips”, *IEEE Transactions on Industrial Electronics*, vol. 56, pp. 4246-4254, 2009.

[37] M. Rahimi, and M. Parniani, “Efficient control scheme of wind turbines with doubly fed induction generators for low voltage ride through capability enhancement”, *IET Renewable Power generation*, vol. 4, pp. 242-252, 2010.

[38] Y. Jin, J. E. Fletcher, and J. O’reilly, “A series dynamic resistor based converter protection scheme for doubly fed induction generator during various fault conditions”, *IEEE Transactions on Energy Conversion*, vol. 25, pp. 422-432, 2010.

[39] J. Morren and S. W. H. de Haan, “Short-circuit current of wind turbines with doubly fed induction generator”, *IEEE Transactions on Energy Conversion*, vol. 22, pp. 174-80, 2007.

[40] J. Lopez, P. Sanchis, X. Roboam, and L. Marroyo, “Dynamic behavior of the doubly fed induction generator during three-phase voltage dips”, *IEEE Transactions on Energy Conversion*, vol. 22, pp. 709-17, 2007.

[41] I. M. de Alegria, J. Andreu, J. L. Martin, P. Ibanez, J. L. Villate, and H. Camblong, “Connection requirements for wind farms: A survey on technical requierements and regulation”, *Renewable and Sustainable Energy Reviews*, vol. 11, pp. 1858-1872, 2007.

[42] E. O. Netz, “Grid Code, High and Extra High Voltage”, *Bayreuth, Germany*, 2006.

[43] X. Dawei, R. Li, P. J. Tavner, and S. Yang, “Control of a doubly fed induction generator in a wind turbine during grid fault ride-through”, *IEEE Transactions on Energy Conversion*, vol. 21, pp. 652-62, 2006.

[44] R. G. de Almeida, J. A. P. Lopes, and J. A. L. Barreiros, “Improving power system dynamic behavior through doubly fed induction machines controlled by static converter using fuzzy control”, *IEEE Transactions on Power Systems*, vol. 19, pp. 1942-50, 2004.

[45] L. Jiaqi, Q. Wei, and R. G. Harley, “Direct transient control of wind turbine driven DFIG for low voltage ride-through”, *IEEE Conference on Power Electronics and Machines in Wind Applications*, Piscataway, NJ, USA, pp. 1-7, 2009.

[46] L. Tian, T. Wang, and W. Wang, “Research on improving the fault ride-through capability wind farm by utilizing STATCOM”, *in Proceedings of the 2011 IEEE International Conference on Advanced Power System Automation and Protection*, Piscataway, NJ, USA, pp. 97-101, 2011.

[47] J. I. Llorente and M. Visiers, “Method and device for injecting reactive current during a mains supply voltage dip”, *Worldwide Patent WO2006/089989*, 2006.

[48] K. E. Okedu, S. M. Muyeen, R. Takahashi, and J. Tamura, “Wind farms fault ride through using DFIG with new protection scheme”, *IEEE Transactions on Sustainable Energy*, vol. 3, pp. 242-254, 2012.

[49] R. Pena, J. C. Clare, and G. M. Asher, “Doubly fed induction generator using back-to-back PWM converters and its application to variable-speed wind-energy generation”, *IEE Proceedings-Electric Power Applications*, Vol. 143, pp. 231-41, 1996.

[50] A. D. Hansen, N. A. Cutululis, H. Markou, P. Sorensen, and F. Iov, “Grid fault and design-basis for wind turbines, Final report, *Rise-R-1714(EN)*, 2010.

[51] A. D. Hansen, N. A. Cutululis, P. Sorensen, and F. Iov, “Mapping of grid faults and grid codes, *Rise-R-1617(EN) Ris National*

Laboratory Technical Universityof Denmark.Roskilde, Denmark, 2007.

[52] W. Qiao, and R. G. Harley, “Grid Connection Requirements and Solutions for DFIG Wind Turbines, *in Proc. IEE Energy 2030 Conference*, Atlanta, GA, USA, 2008.

[53] O. S. Adagha, “Review of grid connection requirements for wind farms in the UK, *school of engineering*, university of Aberdeen Kings College, Aberdeen, AB243FX.UK.

[54] M.H.J. Bollen, “Understanding Power Quality Problems, *IEEE Press*, New York, NY, 2000.

[55] W. Christiansen and D. T. Johnsen, “Analysis of requirements in selected Grid Codes, [Online]. Available: http://www.frontwind.com.

[56] Parsons, “Grid Impacts of Wind Power: A Summary of Recent Studies in the United States, *Wind Energy*, vol. 7, pp. 87-108, 2004.

[57] T. Lund, P. Sorenson and J. Eek, “Reactive power capability of a wind turbine with doubly fed induction generator, *Wind Energy* , vol. 10, no. 4, pp. 379-394, 2007.

[58] D. Santos-Martin, S. Arnaltes, and J.L. Rodriguez-Amenedo, “Reactive power capability of doubly fed asynchronous generators, *Electric Power Systems Research* , vol. 78, pp. 1837-1840, 2008.

[59] G. Michalke, “Voltage grid support of DFIG wind turbines during grid faults”, *in Proc. European Wind Energy Conference and Exhibition*, 2007.

[60] E. Tremblay, A. Chandra, and P. Lagace, “Grid-side converter control of DFIG wind turbines to enhance power quality of distribution network”, *in Proc. IEEE Power Engineering Society General Meeting* , 2006.

[61] S. Zhao, N. C. Kumar, "Behavior of doubly-fed induction generator unit during system disturbance", *in proc. Power Engineering Conference*, pp. 1-6, 2008.

[62] I. Erlich, J. Kretschmann, J. Fortmann, S. Mueller-Engelhardt, and H. Wrede, "Modeling of wind turbines based on doubly-fed induction generators for power system stability studies, *IEEE Transactions on Power System*, vol. 22, no. 3, pp. 909-919, 2007.

[63] J. Morren and S. W. H. de Haan, "Short-circuit current of wind turbines with doubly fed induction generator, *IEEE Transactions on Energy Conversion*, vol. 22, no. 1, pp. 174-180, 2007.

[64] P. Zhou and Y. He, "Control strategy of an active crowbar for DFIG based wind turbine under grid voltage dips, *in proc. Int. Conf. Electr. Mach. Syst.*, Seoul, Korea, 2007.

[65] M. Rodrguez, G. Abad, I. Sarasola, and A. Gilabert, "Crowbar control algorithms for doubly fed induction generator during voltage dips, *in proc. European Conference Power Electronic Application*, Dresden, Germany, 2005.

[66] I. Erlich, H. Wrede, and C. Feltes, "Dynamic behavior of DFIG-based wind turbines during grid faults, *in proc. the Power Conversion Conference*, Nagoya, Japan, 2007.

[67] J. F. Conroy and R. Watson, "Low-voltage ride-through of a full converter wind turbine with permanent magnet generator, *IET Renew. Power Gener.*, vol. 1, no. 3, pp. 182-189, 2007.

[68] J. B. Ekanayake, L. Holdsworth, N. Jenkins, "Comparison of 5^{th} order and 3^{rd} order machine models for doubly fed induction generator (DFIG) wind turbines". *Electr. Power Syst. Res.*

[69] V. Akhmatov and H. Knudsen, "An aggregate model of a grid-connected, large-scale, offshore wind farm for power stability investigations-importance of windmill mechanical system, *International Journal of Electrical Power & Energy Systems*, vol. 24, no.

9, pp. 709-717, 2002.

[70] V. Akhmatov, H. Knudsen, and H. Nielsen, “Advanced simulation of windmills in the electrical power supply, *International Journal of Electrical Power & Energy Systems*, Elsevier, vol. 22, no. 6, pp. 421-434, 2000.

[71] Y. Chi, Y. Liu, W. Wang, and H. Dai, “Voltage stability analysis of wind farm integration into transmission network”, *in International Conference on Power System Technology*, pp. 17, 2006.

[72] Y. Lei, A. Mullane, G. Lightbody, and R. Yacamini, “Modeling of the wind turbine with a doubly-fed induction generator for grid integration studies”, *IEEE Transaction on Energy Conversion*, vol. 21, no. 1, pp. 257-264, 2006.

[73] T. V. Custem and C. D. Vournas, “Voltage stability of the electric power systems”, *Norwell: Kluwer Academic* 1998.

[74] A. Berizzi, “The Italian 2003 blackout, *in proc. IEEE Power Engineering Society General Meeting*, Denver, CO, pp. 1673-1679, 2004.

[75] B. A. Foss, and S. Aam: “Regulating river flow”, *Hydro Review*, pages 82-89, 1991.

[76] C. E. Garcia, D. M. Prett and M. Morari, “Model predictive control: Theory and practice, A survey”, *Automatica*, vol. 25, no. 3, pp. 335-348, 1989.

[77] G. Glanzmann, M. Siebenthal, T. Geyer, G. Papafotiou and M. Morari, “Supervisory water level control for cascaded river power plants”, *In Proceedings of the International Conference on Hydropower*, Stavanger, Norway, 2005.

[78] J. M. Maciejowski, “Predicitive control with constraints”, *Prentice-Hall, Pearson Education Limited*, Harlow, UK, 1^{st} edition, 2002.

[79] D. Q. Mayne, J. B. Rawlings, C. V. Rao and P. O. Scokaert, “Constrained Model predictive control: stability and optimality”, *Automatica*, vol. 36, no. 6, pp. 789-814, 2000.

[80] B. Boukhezzar, L. Lupu, H. Sigurdidjane, and M. Hand, “Multivariable control strategy for variable speed, variable pitch wind turbines”, *Renewable Energy*, vol. 32, pp. 1273-1287, 2007.

[81] L. Xu and C. Wei, “Torque and reactive power control of a doubly fed induction machine by position sensorless scheme, *IEEE Transactions on Industry Applications*, vol. 31, no. 3, pp. 636-642, 1995.

[82] L. H. Hansen, L. Helle, F. Blaabjerg, E. Ritchie, S. Munk-Nielsen, H. Bindner, P. Sorensen, and B. Bak-Jensen, “Conceptual survey of generators and power electronics for wind turbines”, *Riso National Laboratory*, Roskilde, Denmark, Tech. Rep. Riso-R-1205(EN), ISBN 87-550-2743-8, 2001.

[83] K. E. Okedu, “A study of wind farm stabilization using DFIG or STATCOM considering grid requirements”, *Journal of Engineering and Technology*, vol. 3, no. 1, pp. 200-209, 2010.

[84] K. E. Johnson, Pao, Y. Lucy, M. J. Balas, and L. J. Fingersh, “Control of variable-speed wind turbines: standard and adaptive techniques for maximizing energy capture”, vol. 26, no. 3, pp. 70-81, 2006.

[85] F. Wu, X. P. Zhang, P. Ju, and M. J. H. Sterling, “Decentralized nonlinear control of wind turbine with doubly fed induction generator”, *IEEE Transactions on Power Systems*, vol. 23, no. 2, pp. 613-621, 2008.

[86] A. Tapia, G. Tapia, J. X. Ostolaza, and J. R. Saenz, “Modelling and control of wind driven doubly fed induction generator”, *IEEE Transactions on Energy Conversion*, vol. 18, no. 2, pp. 194-204, 2003.

[87] J. B. Ekanayake, L. Holdsworth, X. Wu and N. Jenkins, "Dynamic modeling of doubly fed induction generator wind turbines", *IEEE Transactions on Power Systems*, vol. 18, no.2, pp. 803-809, 2003.

[88] M. V. A. Nunes, J. A. Peas, H. H. Zrn, U. H. Bezerra and R. G. Almeida, "Influence of the variable-speed wind generators in transient stability margin of the conventional generators integrated in electrical grids", *IEEE Transactions on Energy Conversion*, vol. 19, no. 4, pp. 692-701, 2004.

[89] L. M. Fernandez, C. A. Garcia, F. Jurado, and J. R. Saenz, "Control system of doubly fed induction generators based on wind turbines with production limits", *IEEE International Conference on Electric Machines and Drives*, pp 1936-1941, 2005.

[90] J. L. Rodriguez-Amenedo, S. Arnalte and J. C. Burgos, "Automatic generation control of a wind farm with variable speed wind turbines", *IEEE Transactions on Energy Conversion*, vol. 17, no. 2, pp. 279-284, 2002.

[91] T. H. Nguyen, D. C. Lee, "Advanced fault ride-through technique for PMSG wind turbine systems using line-side converter as STATCOM", *IEEE Transactions on Industrial Electronics*, vol. 60, no. 7, pp. 2842-2850, 2013.

[92] M. Mirzaei, N. Kjolstad, and H. H. Niemann, "Robust model predictive control of a wind turbine", *in proc. American Control Conference*, pp. 4393-4398, Canada, 2012.

[93] J. Richalet, "Industrial applications of model based predictive control", *Automatic*, vol. 29, no. 5, pp. 1251-1274, 1993.

[94] K. Edlund, J. D. Bendtsen, S. Borresen, and T. Molbak, "Introducing model predictive control for improving power plant portfolio performance", *in Proc.* 17^{th} *World Congress of The Int. Federation of Automatic Control (IFAC)*, pp. 6986-6991, 2008.

[95] W. Qi, J. Liu, X. Chen, and P. D. Christofides, "Supervisory predictive control of standalone wind/solar energy generation systems", *IEEE Transactions on Control Systems Technology*, vol. 19, no. 1, pp. 199-207, 2011.

[96] Z. Yi, D. Kullmann, A. Thavlov, O. Gehrke, and H. W. Bindner, "Application of model predictive control for active load management in a distributed power system with high wind penetration", *IEEE Transactions on Smart Grids*, vol. 3, no. 2, pp. 1055-1062, 2012.

[97] Z. Yang, Y. Li, and J. E. Seem, "Model predictive control for wind turbine load reduction under wake meandering of upstream wind turbines", *American Control Conference*, pp. 3008-3013, 2012.

[98] M. Geyler and P. Caselitz, "Robust multivariable pitch control design for load reduction on large wind turbines", *Journal of Solar Energy Engineering*, vol. 130, no. 3, 2008.

[99] F.D. Bianchi, R.J. Mantz and C.F. Christiansen, "Power regulation in pitch-controlled variable- speed WECS above rated wind speed", *Renewable Energy*, vol. 29, pp. 1911-1922, 2004.

[100] M. Soliman, O. P. Malik, and D. T. Westwick, "Multiple model MIMO predictive control for variable speed variable pitch wind turbines", *in proc. American Control Conference*, pp. 2778-2784, 2010.

[101] G. Valverde,and T. V. Cutsem, "Model predictive control of voltages in active distribution networks", *IEEE Transactions on Smart Grid*, pp. 1-10, 2013.

[102] A. Borghetti, M. Bosetti, S. Grillo, S. Massucco, C. A. Nucci, M. Paolone, and F. Silvestro, "Short-term scheduling and control of active distribution systems with high penetration of renewable resources", *Syst. J.*, vol. 4, no. 3, pp. 313-322, 2010.

[103] J. M. Maciejowski, "Predictive control with constraints", *Englewood Cliffs* , NJ, USA: Prentice-Hall, 2002.

[104] A. Khatamianfar, A. Savkin, V. G. Agelidis, "Improving wind farm dispatch in the australian electricity market with battery energy storage using model predictive control", *IEEE Transactions on Sustainable Eneregy*, vol. 4, no. 3, pp. 745-755, 2013.

[105] T. V. Cutsem and C. Vournas, "Voltage stability of electric power systems", *Norwell, MA, USA*: Kluwer, 1998.

[106] B. Gong, and I. A. Hiskens, "Two-stage model predictive control for voltage collapse prevention", *In Proc.* 40^{th} *North Amer. Power Symp.*, pp.1-7, 2008.

[107] www.ramblingsdc.net/Australia/WindWA.html

[108] http://cleanenergyaustralareport.com.au/technologies/wind-2

[109] http://adl.brs.gov.au/data/warehouse/peaerad9aae002/aeraCh08.pdf

[110] www.science.org.au/reports/documents/Ausewnewableenergyfuture.pdf

[111] I. Muteanu, A. I. Bratcu, and N. A. Cutululis, "Optimal control of wind energy systems", *London, Springer*, 2008.

[112] T. V. Cutsem, "Voltage instability: Phenomenon, countermeasures and analysis methods, *Proceedings of the IEEE*, vol. 88, no. 2, pp. 208227, February 2000.

[113] P. Kundur, "Power system stability and control", *New York: Mcgraw-Hill*, 1994.

[114] H. D. Tuan, A. Savkin, N. T. Nguyen, and H. T. Nguyen, "Decentralised model predictive control with asymptotically positive realness", *in proc. IEEE International Conference on Control and*

Automation, pp. 822-827, 2013.